PNC TN9410 96-011

Pu Vector Sensitivity Study for a Pu Burning Fast Reactor

January 1996

O-ARAI ENGINEERING CENTER
POWER REACTOR AND NUCLEAR FUEL DEVELOPMENT CORPORATION

動力炉・核燃料開発事業団（Power Reactor and Nuclear Fuel Development Corporation）

COMMERCIAL PROPRIETARY

PNC TN9410 96-011

January, 1996

Pu Vector Sensitivity Study for a Pu Burning Fast Reactor

Stuart Hunter*

Abstract

This study used a 'pancake' type fast reactor core design of 600 MW(e) which had been optimised for Pu burning with a feed Pu vector appropriate to once-through irradiation of MOX fuel in a PWR. The purpose of the study was to investigate the feasibility of using different qualities of Pu vector within the same basic core design. In addition to the reference (once-through) Pu vector, two extreme Pu vectors were examined: high quality Pu from military stockpiles; low quality Pu corresponding to the equilibrium point of multiple recycling in a Pu burning fast reactor.

The calculations used a 2D R-Z model. The cell lattice code SLAROM, the diffusion & burnup code CITATION and the perturbation code PERKY were used. Cross-section data was taken from JENDL-3.2.

The key results for the reference Pu vector case were a reactivity loss per cycle of 4.304% and the main safety parameters, a Na void worth of 1.631% and a Doppler constant of -0.00573 (a ratio of -285). The reactivity loss and void-to-Doppler ratio were used as targets for the calculations with the other Pu vectors.

For the high quality Pu vector it was necessary to introduce an amount of diluent material into the core, to allow criticality criteria to be met. Several different classes of diluent were examined: increased fuel pin voidage, materials transparent to neutrons, moderators and neutron absorber. Compared with the initial 'reference' Pu vector, with absorber as diluent there was an improvement in the reactivity loss per cycle (down to ~3.4%) but a degradation in the main safety parameters with the void:Doppler ratio around -2000. With any of the other materials used as diluent the situation was reversed, with the reactivity loss increased to around 6% but Na void and Doppler improved to a ratio around -20.

A mixture of absorber with another diluent material was shown to balance the above effects. A diluent of $ZrH_{1.7}$ together with $^{10}B_4C$ was capable of producing an improvement over the 'reference' case in the key parameters. It also demonstrated the feasibility of enhancing the Pu burning rate by using a uniform Pu enrichment, the diluent fraction being used to control the inner/outer zone balance. A diluent of B_4C, the ^{10}B fraction adjusted to control the absorber/moderator balance, produced results a little inferior to the reference case; a small reduction in cycle length, from 6 to 5.3 months, would allow the reference case to be matched.

For the low quality Pu vector, for the criticality criteria to be met it was necessary to increase the pin size and hence the fuel inventory: this was preferrable to other options such as increasing

* Reactor Physics Research Section, Advanced Technology Division, O-arai Engineering Center, PNC, Japan

Pu enrichment or greatly reducing cycle length. The results showed a degradation of Na void and Doppler relative to the reference case (a void:Doppler ratio of -660), but a reduction in the reactivity loss (to 2.9%). The introduction of a non-absorber as diluent (requiring further pin size increase) was shown to be capable of producing key parameters that matched the reference case: for $ZrH_{1.7}$ as diluent a pin volume increased by a factor x1.5 was necessary, though for Al_2O_3 (typical of other materials) a pin size x2.2 was needed.

The effect of pin size increases of x1.5 and x2.2 on the reference and high quality Pu vectors was examined. Two diluent materials were assessed, a mix of $^{10}B_4C$ with ZrH, B_4C as both moderator and absorber; this latter case was typical of other diluent materials. In all cases it was possible to produce key parameters within the reference case values. However, for the cases with B_4C as moderator the pin ratings were significantly above a 430 W/cm limit, unless a large proportion of the diluent material was incorporated into the fuel pellets rather than in separate pins.

The results of the study provide support for the use of a single reactor design for burning Pu of all compositions. The worth of control rods will be reduced by the requirement to use $^{10}B_4C$ absorber as diluent for the better quality Pu vectors; further calculations, using 3D models, are required to assess the adequacy of shutdown margins. ZrH is identified as a preferred diluent material: if it could not be used, then diluent (possibly in the form of increased void) would have to be incorporated within fuel pellets if pin ratings were to be kept within limits; alternatively, it would be necessary to adopt a S/A design which allowed for different pin/pellet sizes for use with the different qualities of Pu. The effect of diluent pins within a fuel S/A, on rating and thermo-hydraulic performance, should be addressed, with particular consideration of whether absorber ($^{10}B_4C$) is in separate pins from other diluent materials.

CONTENTS

LIST OF TABLES

LIST OF FIGURES

1 INTRODUCTION

A significant area in the nuclear fuel cycle which has yet to be definitively resolved is the final disposal of long lived radiotoxic waste. It is undesirable from ethical, political, ecological and economic viewpoints to leave unnecessarily large stocks of materials which may remain a potential hazard, whether real or perceived, for many future generations. Transmutation of those radiotoxic nuclides - plutonium (Pu), minor actinides and long lived fission products - which produce the long term radiotoxicity of the waste stream, is an attractive option for greatly reducing the long term waste produced by the nuclear fuel cycle.

Considerable investigation has been taking place, both in Japan[1-1 to 1-5] and elsewhere[1-6 to 1-9], into the use of fast reactors to transmute Pu, minor actinides and long lived fission products. The hard neutron spectrum in a fast reactor makes it particularly suitable for such a transmutation role. When Pu and minor actinides are transmuted (fissioned) in a fast reactor, they become a valuable fuel resource rather than an waste product liability.

This report presents the results of a reactor physics study that was undertaken to investigate the feasibility, within a single design of core, for a Pu burning fast reactor to utilise the full range of Pu isotopic compositions that may be available. The potential flexibility of a fast reactor to burn all grades of Pu is a further advantage over other methods of Pu transmutation - at the one extreme it allows stockpiles of military Pu to be used directly, whilst at the other the use of multiple recycling can minimize the Pu remaining in the waste stream.

The study used a 600 MW(e) fast reactor core design [1-10] that had been optimized for Pu burning with a Pu vector appropriate to once-through irradiation of MOX fuel in a PWR[1-10] - this is used as a 'reference' case in this study. Two extreme Pu vectors were examined, they are those appropriate to military Pu and an equilibrium Pu composition calculated for multiple recycling in a Pu

burning fast reactor[1-11], referred to below as 'high' and 'low' quality Pu. All three Pu compositions are shown in Table 1.1.

The study was limited to the consideration of MOX fuel in the Pu burning core; advanced fuel concepts such as nitride or Pu without U fuel are beyond the scope of this study. Fuel solubility considerations during reprocessing impose a limit on the Pu enrichment of 45% - a lower peak enrichment is undesirable, since Pu burning rate is primarily a function of Pu enrichment[1-12] so the Pu burning rate would also be lower. Inherent in the aims of the study is the requirement to use a fixed fuel geometry. The reference case fuel cycle has a cycle length of 6 months, any shorter cycle would be undesirable from an economic standpoint.

The analysis was focused on two particular areas of the core characteristics. The high Pu enrichment in a Pu burner core causes there to be a comparatively large reactivity swing over an irradiation cycle - it is to compensate for this that the reference case has a cycle length of only 6 months. The second area comprises those parameters that relate to reactor safety, in particular Na void worth and Doppler coefficient.

Table 1.1 Isotopic compositions of the three Pu vectors (w/o)

Pu Quality	Pu 238	Pu 239	Pu 240	Pu 241	Pu 242	Am 241
High (military)	0.0	94.0	6.0	0.0	0.0	0.0
Reference (once through)	1.8	58.2	22.3	11.1	5.5	1.1
Low (multi-recycled)	3.4	32.6	39.8	8.0	15.4	0.8

2 REFERENCE CORE DESIGN

For the purposes of this study many of the parameters of the reference core were taken as fixed, since the aim of the calculations was to show flexibility within a given core design. The details of the basic core design were taken from Reference 1-10 and are summarized in Table 2.1.

The reference core design has a power of 600 MW(e), 1560 MW(th). There are no breeder regions and a 'pancake' style of core is adopted: the active core has a height of 0.6 m and radius 4.0 m (this core shape has benefits in terms of Na void characteristics).

The core consists of 541 fuel S/As and 36 control rod S/As, it is surrounded by 270 shielding S/As; the positions of control rod S/As and their distribution between control and shutdown duties are fixed; the reference core has 295 S/As in the inner fuel zone (though the enrichment zone boundary could, in principle, be altered for different Pu vectors). The core layout is shown in Figure 2.1.

The S/A geometry is fixed, with a hexagonal (a/f) pitch of 158.1 mm, 217 pins of 5.778 mm outer diameter and 0.4185 mm clad thickness, fuel pellets of 4.781 mm diameter . The S/A wrapper has a thickness of 3.9 mm and there is an inter-wrapper gap of 5.8 mm. There is no wire round the pins, which are instead held in place by grids. This design results in the fuel S/As having the following volume fractions: fuel pellet 18.00%, steel 16.32%, Na 64.46% (grids were not taken into account in the reference case).

The fuel pellet is MOX with 90% of theoretical density; the fuel has an O:M ratio of 1.98. The uranium contains 0.3% ^{235}U (w/o). The Pu enrichment depends on the calculation; for the reference case it is 37.5% and 45% in the inner and outer zones respectively. The Pu vector compositions used, including ^{241}Am, are shown in Table 1-1.

For the reference case the fuel has an irradiation cycle length of 6 months and is irradiated for a total of 4 batches.

The shield, rod follower and rod absorber regions are characterized by their volumetric compositions. The radial and axial shields are a uniform composition of 20% Na and 80% steel; the followers 90.7% Na and 9.3% steel; the absorbers 42.5% Na, 22.6% steel and 33.3% B_4C. The axial shields extend for 0.3 m above and below the active core.

All the steel is taken to be SUS316, with a density of 7.98 g/cc and a composition of Fe 65.5%, Cr 17.0%, Ni 13.5%, Mo 2.5%, Mn 1.5%. The B_4C in the absorber has 92% ^{10}B and 95% of theoretical density. An Na density of 0.837936 g/cc was used, this corresponds to a temperature of 476C. All other density data was taken, either explicitly or implicitly, from those encoded in the PENCIL[2-1] computer program.

Table 2.1 Main parameters of reference core

Reactor Power	600 MWe / 1560 MWth
Core Diameter	4.0 m
Core Height	0.6 m
Fuel Type	MOX
Pu Enrichment	37.5% (inner core) 45.0% (outer core)
Numbers of S/As	Inner Core 246 Outer Core 295 Main Rods 27 Backup Rods 9
Core Volume Fractions	Fuel 18.00% Steel 16.32% Coolant 64.46%
No. of Pins per S/A	217
Fuel Pellet Diameter	4.781 mm
Clad Thickness	0.4185 mm
Clad Outer Diameter	5.778 mm
Wrapper Thickness	3.9 mm
Inter-Wrapper Gap	5.8 mm
Core Pitch	158.1 mm (a/f)
Pin Support	grids
Cycle Length	6 months
Fuel Irradiation	4 batches

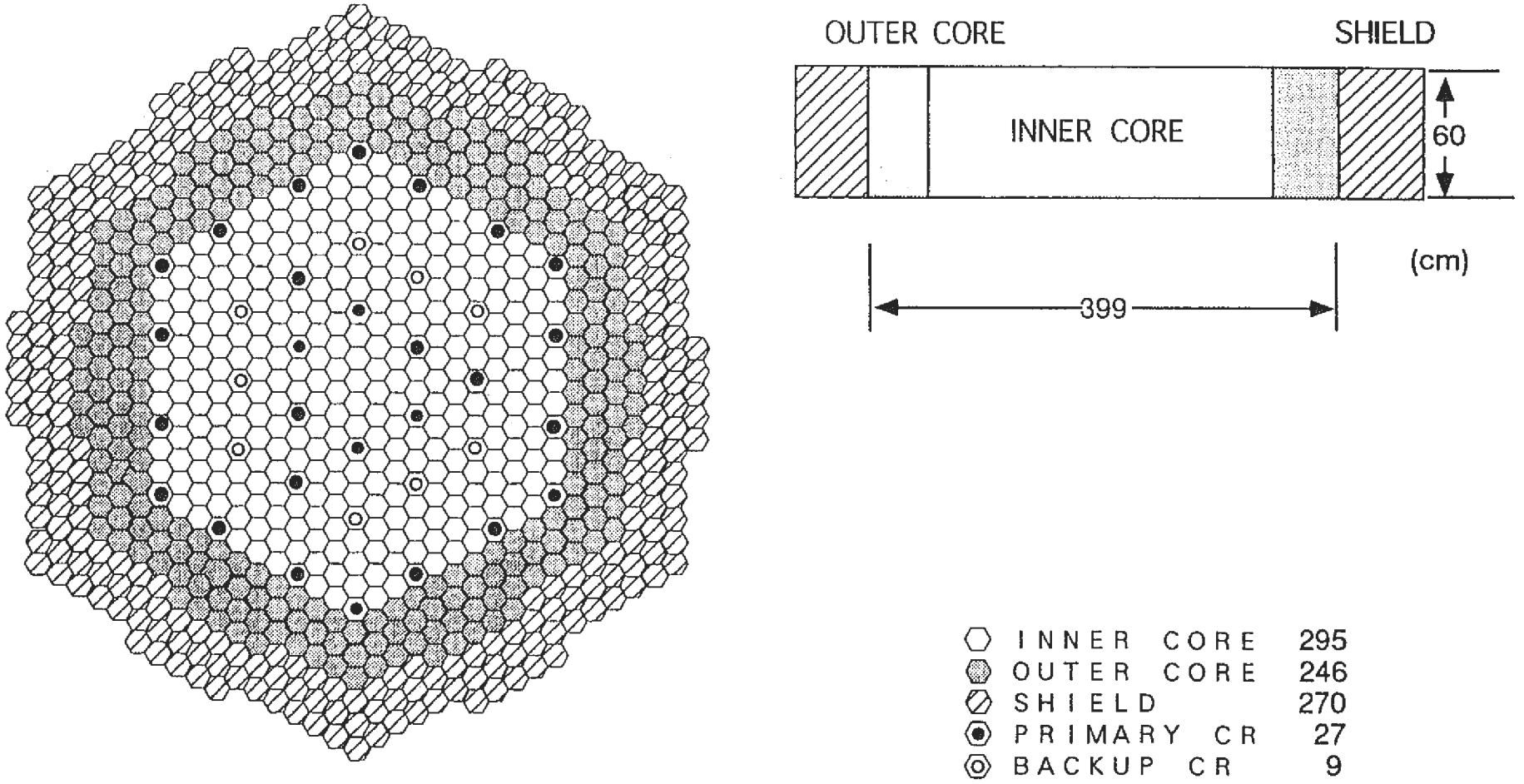

Fig. 2.1 Configuration of a Pu burner core (600MWe, MOX fuel)

3 CALCULATION METHODS

Possible modifications to the reference core and fuel cycle design, to adapt it to the 'high' and 'low' quality Pu vectors, were somewhat restricted. The active core size and S/A design had to be constant for all 3 vectors - the S/A pitch and thermohydraulic characteristics must be the same, for the present the latter was assumed to require a fixed pin size. The peak Pu enrichment in the core was fixed at around 45%: any higher level would cause problems with fuel solubility during reprocessing[1-11]; lower values are undesirable since the rate of Pu burning is roughly proportional to the Pu enrichment[1-12].

Reductions in cycle length below the reference value of 6 months were considered highly undesirable, because of the economic consequences of more frequent refuellings. The high Pu enrichment causes a large loss of reactivity with burnup, it was to combat this that the reference case had adopted a cycle length of just 6 months. The possibility of controlling reactivity loss by using a small number of poisoned S/As, present for just the first part of each cycle, was not considered because of the economic consequences of doubling the number of reactor shutdowns. Such an approach to reactivity control in a Pu burning in a fast reactor has been examined in other studies[1-12].

The number of cycles for which the fuel is irradiated was open to variation. The position, and even the number, of enrichment zone boundaries could have been altered, though this option was not generally considered in this study. The main parameter used to modify the core design was the introduction of a diluent material to replace a fraction of the fuel within the pins. Absorber, moderators and materials transparent to neutrons (including 'void') were assessed as diluent materials. The fraction of diluent was used as a variable to control the core reactivity - to produce a target k_{eff} of 1.0048 at EOEC with all rods out. The balance of peak ratings was controlled by varying the inner zone Pu enrichment, relative to an outer zone value of 45%.

The assessment used a calculational route set up at PNC[3-1] specifically for use in studies on Pu, minor actinide and long-lived fission product burning in fast reactor cores. There are 3 main programs used in the route: SLAROM[3-2] is a cell lattice program, the route uses a homogeneous cell model to produce macroscopic cross-section data for all materials; CITATION[3-3] performs eigenvalue and depletion calculations using a finite difference representation of diffusion theory, the route adopts a 2D R-Z geometry; PERKY[3-4] performs perturbation and associated calculations, the route includes both exact and 1'st order perturbation calculations. The route includes a number of small programs to facilitate the interface between the various components, the most important of these are part of JOINT[3-5].

The calculations were used to produce values of various parameters for fuel cycle equilibrium. The rate of reactivity loss has already been noted as particularly significant for Pu burning cores; the rate of Pu burning is also important, since the aim is to maximise it. Peak linear ratings were calculated, they were considered against a limit of 430 W/cm[3-6]. The mean fuel irradiation was calculated, though no irradiation or clad damage limit was explicitly considered in the study. Values were calculated for four parameters of particular consequence to the safety analysis of the core: Na void worth; Doppler coefficient; prompt neutron lifetime (τ) and delayed neutron fraction (β) - they were calculated at EOEC, since the spectrum effects of fuel burnup result in EOEC values being more severe than those for BOEC. The components of Na void and Doppler were also calculated.

Within this study, the core calculations for the high and low quality Pu vectors were assessed against the initial reference Pu calculation: it was aimed to demonstrate that core designs could be produced that were no worse than the reference core. In comparing the designs, the key parameters considered were the rate of reactivity loss and the safety parameters. In fault transients where Na boiling occurs, the Na void effect acts to increase the severity of the fault whilst the (negative) Doppler effect acts to mitigate the fault; in non-boiling faults just the Doppler effect is relevant. For both Na void and Doppler, the parameter should be divided by

delayed neutron fraction (β) to facilitate a true comparison between different cores. The speed, and hence the severity, of a transient is related to the inverse of prompt neutron lifetime (τ). For assessing the different cores the ratio

Na void worth : Doppler coefficient

was adopted as a simple comparison measure. For the limited number of cases where values of delayed neutron fraction and prompt neutron lifetime were available, the following secondary safety comparators were also used -

from boiling faults - $\frac{void}{doppler.\tau}$

from non-boiling faults - $\frac{\beta}{doppler.\tau}$

It is noted that the import of the rate of reactivity loss is in its effect on shutdown margins; calculations of shutdown margins require the use of 3D calculations and as such were not included in the current analysis. It is intended that shutdown margin calculations will be presented in a later report. It is anticipated that where some absorber is used as a diluent material, this will have a deleterious effect on the shutdown margin; calculations for the reference core[1-10] show some scope to allow for possible reductions in margin.

3.1 CALCULATIONAL ROUTE

The calculational route is basically that described in reference 3-1. The main constituent programs are the lattice cell program SLAROM[3-2], the CITATION[3-3] diffusion program used for eigenvalue and depletion calculations, the PERKY[3-4] perturbation program. The only significant deviations from the route in reference 3-1 are in the number of meshes used to represent the core and in the number of energy groups used in certain of the perturbation calculations - justification for these changes is given in Section 3.2. The following paragraphs give a brief outline of the calculational route.

The cross-section data used for the main calculations was taken from a library (JFS3-J3) that was condensed from JENDL-3.2[3-7] to 70 energy groups for a typical fast reactor spectrum. Certain of the calculations used cross-section data condensed to 7 energy groups; separate 7-group cross-section datasets were produced for each different diluent material type for each of the three Pu vectors, they were not recalculated for variations in the proportions of diluent in the core.

A 'basic' calculation sequence comprises 3 parts: calculations which reference 3-1 refers to as PENCIL, CITDENS and SLAROM-JOINT-CITATION (S-J-C). PENCIL[2-1] is a program which takes data in the form of core parameters and creates an equivalent number density input file for the program CITATION, which is run embedded within PENCIL. The PENCIL calculation starts with a clean core and models depletion and refuelling for 2 or 3 cycles longer than a complete irradiation cycle, with one depletion timestep per cycle, so the final timestep approximates to fuel cycle equilibrium. The PENCIL calculation carries this out not once but a series of times, iterating Pu enrichments to achieve a defined EOEC k_{eff} and inner/outer zone rating balance - a CITATION input dataset for the final converged Pu enrichments is saved. CITDENS consists of a single CITATION calculation, repeating the final iteration of the preceeding PENCIL calculation, but producing an output file of material number densities for each stage in the calculation. Both PENCIL and CITDENS calculations use 7-group cross-sections; macroscopic cross-section data is calculated within CITATION, from number densities and a 7-group microscopic cross-section library file and for a homogeneous representation within each mesh. S-J-C takes as input number densities produced by CITDENS, for either BOEC or EOEC: a SLAROM calculation produces 70-group macroscopic cross-section data from the input number densities and the 70-group microscopic cross-section library; a CITATION eigenvalue calculation is run. The 70-group S-J-C calculation is used to produce a more accurate core snapshot based on the number densities from the 7-group burnup calculation. S-J-C calculations for BOEC and EOEC conditions provide the reactivity loss per cycle from the difference in their k_{eff} values; variations with core temperature or Na number density

modified provide values of k_{eff} from which Doppler coefficient and Na void worth are calculated.

Where it was required to produce a new 7-group microscopic cross-section dataset for an altered core composition, the following procedure was used. One of the JOINT interface programs that is part of S-J-C provides a condensation of microscopic cross-sections from 70 to 7 groups, for the condition calculated by S-J-C. An iterative series of 'basic' calculations were performed, the Pu enrichments in PENCIL were fixed and at each new iteration the condensed 7-group microscopic cross-sections produced by the previous S-J-C were used as input to the following PENCIL and CITDENS; the iterations continued until the equilibrium conditions calculated by PENCIL converged, typically after 3 iterations.

To calculate the mass balance of the fuel for the equilibrium cycle a short program, MASSN[3-1], is part of the calculational route; it is usually incorporated within a 'basic' calculation sequence. This program uses the number density file created by the CITDENS part of a 'basic' calculation. The Pu burning rates are calculated on the basis of a 100% load factor and making no adjustments for minor actinides generated during irradiation or for ^{241}Pu decay during reprocessing.

The perturbation program PERKY is used for four types of calculations: 70-group exact perturbation calculations of Na void, using macroscopic cross-section data; 18-group 1'st order perturbation calculations of Doppler, using microscopic cross-section data and producing results for each isotope; 70-group prompt neutron lifetime calculations; 18-group delayed neutron fraction calculations. To produce data necessary for the PERKY calculations, a series of one SLAROM and four CITATION calculations are run. The SLAROM calculation takes the EOEC number densities produced by the CITDENS part of a 'basic' calculation and uses them to create a file of 70-group microscopic and macroscopic cross-section data for three reactor states: the normal condition; the Doppler condition of core temperatures increased 500° isothermally; the Na void condition of core Na number density reduced to zero. There are three 70-group JOINT-CITATION calculations, one for each of the three reactor states for which SLAROM created cross-sections - between them these

calculations produce files of: 70-group direct and adjoint fluxes for the normal state; 70-group (direct) flux for the Na void state; microscopic and macroscopic cross-section data condensed to 18 energy groups, for both normal and Doppler states. An 18-group CITATION calculation for the normal state is used to produce an 18-group (direct) flux file.

3.2 DETAILS OF CALCULATIONS

The calculational route as described in reference 3-1 uses a 2D R-Z model which represents just half the reactor height, with a reflective boundary at the core centre plane; separate number densities are only represented for 5 regions - the 2 core enrichment zones, upper and radial shields and rod follower. Because only half core height is represented, no absorber rods are modelled. (In the CITATION depletion calculations within PENCIL, for both fuel regions the number density of each batch is stored separately but smeared macroscopic cross-sections are calculated for the region.)

For the current study, the mesh detail was increased; results supporting this change are given in Section 3.2.1. The number of material regions was increased from 5 to 31, 20 of these were used to represent the core. In order to prevent cross-section datafiles becoming unmanageably large, where the 'basic' calculation (described in Section 3.1) was used in the production of newly condensed 7-group cross-section libraries, the S-J-C part of the calculation was carried out using the original 5 region number density structure. Thus all the 7-group cross-section libraries used were based on the original 5 region structure.

The Na void PERKY calculations were done for 70 energy groups, rather than for 18 groups as in reference 3-1; results supporting this change are given in Section 3.2.2. The perturbation calculations had to be modified to accommodate the change to 31 material regions: in the SLAROM calculation, whilst 70-group macroscopic cross-section data was stored for all 31 materials in each of the normal, Doppler and Na void states, the microscopic data was only stored for a single (core) region for each of the three

states. This change was necessary to avoid unmanageably large datafiles. A minor error was introduced, since all the microscopic data stored was for the core temperature - it would have been more appropriate to store microscopic cross-section data for the three temperatures used: 1373 K for the core, altered to 1873 K for Doppler, and 703 K for shield and follower. An examination of the results found no significant effects from this temperature error.

The main mechanism for adapting the reference core design to the different Pu vectors was the replacement of part of the MOX fuel material by a diluent. The replacement material might be placed in separate S/As, in unfuelled pins within each S/A, or mixed in each fuel pellet - in the case of using 'void' as diluent, the latter option could be implemented by using hollow fuel pellets. Diluent mixed in the fuel pellets would be preferable from the consideration of pin ratings, but chemical compatability and fuel pellet properties may preclude such an option.

In this study the fuel macroscopic cross-sections were calculated on the basis of a homogeneous cell model. This will more nearly represent the diluent mixed in fuel pellets than it does separate diluent pins, though it is believed that for current purposes the calculations adequately represent both situations. For separate diluent S/As, it would be appropriate to treat the diluent as completely separate from the core for the purposes of calculating number densities and cross-sections, in a manner similar to rod absorber/follower S/As. Whilst it would be possible to represent diluent S/As in R-Z geometry, they have the potential to induce considerable rating variations, both between and within S/As; 3D calculations would be required for proper modelling of diluent S/As, they have therefore not been included in the current study. It is noted that the self-shielding effect of concentrating the diluent in S/As would increase the amount of diluent required, this would have the effect of further increasing pin ratings.

There is one major difference between having diluent mixed in fuel pellets and in separate pins (or S/As): for a given volumetric heat rate the fuel pin linear rating in the former case will be (1-diluent fraction) times that in the latter. The results in this report give two types of pin rating value: 'type A' for the diluent

material mixed in the fuel pellet and 'type B' for diluent placed in separate pins.

Where the diluent includes absorber (^{10}B in B_4C) the use of an homogeneous cell model is not strictly appropriate; however, this can be compensated for by using a lower ^{10}B fraction in the calculation than would be used in practise (see Section 5.4). It is noted that the CITATION depletion calculation includes burnup of any ^{10}B in the diluent.

The volume fractions of fuel and diluents in a S/A are given in terms of numbers of pins (out of a total of 217). This same measure is used independant of whether the diluent and fuel materials are actually segregated into different pins.

The calculations used the cold dimensions of the core. Since the study is only comparing different core options, this simplification is not important.

In the PENCIL calculations the free variables (generally the Pu enrichments) were used to obtain a balance of inner and outer zone peak linear ratings at EOEC. Since absorber rods are not modelled, ratings (and k_{eff}) are not balanced at BOEC, so the peak BOEC linear ratings may be overestimated. EOEC ratings were balanced because there is more likely to be scope at BOEC for the use of differential rod insertions to balance ratings than there is at EOEC. The R-Z calculations cannot fully represent the radial rating variations between and within S/As, this may lead to the peak ratings being to some extent underestimated; any effect will be most significant should diluent be placed in separate S/As. The 70-group S-J-C calculations will produce a more accurate calculation of ratings for a given core condition than will the 7-group PENCIL calculation. However, core conditions were chosen to give balanced EOEC ratings in PENCIL, they may not remain so balanced in the equivalent S-J-C calculation, so unless calculations are for a fixed core condition comparisons were made using ratings from the 7 group PENCIL calculations.

The prompt neutron lifetime and delayed neutron fraction calculations are not strictly part of the calculational route of

reference 3-1. The data used in the delayed neutron fraction calculations are shown in Tables 3.1 and 3.2, the yield fractions are taken from references 3-8 and 3-9 and the delayed neutron spectra from reference 3-10.

3.2.1 MESH SIZE ASSESSMENT

The original calculational route of reference 3-1 adopts a core number density representation of 5 radial and 3 axial meshes in the PENCIL and CITDENS calculations but only 2 meshes, one per Pu enrichment zone, in the S-J-C calculations. (All axial mesh sizes are given for the half core height.) The flux representation uses 60 radial and 6 axial meshes. The equivalent figures for the calculations in reference 1-10 for the reference core are 12 radial and 2 axial number density meshes, 40 radial and 6 axial flux meshes.

In view of the enhanced axial leakage in the pancake core design under assessment, and the importance of that leakage to the Na void worth, it was judged necessary to ensure that the calculations were done with sufficient detail in the axial mesh representation.

A series of calculations were done in which the effects of increasing the number of axial meshes was examined; this included altering the S-J-C calculations to have the same mesh as PENCIL and CITDENS. The calculations were for the reference quality Pu vector of reference 1-10, the Pu enrichments are fixed at 37.5 and 45.0% for the inner and outer cores respectively. This case is examined in further detail in Chapter 4. As well as a coarser mesh based on references 1-10 and 3-1, and a more refined mesh that was adopted as standard for the calculations in this study, a yet finer mesh was examined, as were intermediate cases where flux and number density meshes were varied independantly. The standard mesh is shown in Figure 3.1, the figure includes shield regions; the core has 10 axial and 39 radial flux meshes, 4 axial and 5 radial number density meshes - the axial number density meshes are graded in size (ratio 4:3:2:1, from the centre outwards). The finer mesh examined was just half that of the standard.

The results of the calculations are shown in Table 3.3; the values are from the 70-group S-J-C calculations. Changing from the coarse mesh of references 1-10 and 3-1, to the standard mesh, causes some significant changes: the Na void worth increases by 40-45%, k_{eff} increases by 0.8-1.4%, Doppler coefficient increases by 2.4-3.4% The further halving of axial mesh sizes has comparatively little effect, Na void reducing by only 1.4% and other parameters showing proportionately smaller effects. These results demonstrate that the reduced axial mesh size adopted as standard was both necessary and adequate.

It is noted that, unlike in the calculational route of reference 3-1, the region above the control rod positions is represented as axial shield rather than rod follower. This was judged a more reasonable assumption, since with control rods fully withdrawn there will be axial shield below the core and absorber above the core. With the above rod material represented as the more transparent follower material the possibility of calculational instability would be increased.

There was a second reason why the axial mesh detail was examined. Calculations undertaken on Pu burning cores as part of the European CAPRA project[3-11] have shown significant increases in the thermal flux, producing appreciable thermal fission close to core boundaries; the effect had the potential to produce anomalous power distributions that increase (and even peak) in the top/bottom meshes of an axial distribution. The enhanced thermal flux at the edge of the core was the result of a combination of effects: dilution in the Pu burner core increased the neutron thermalization within the core; the shield/reflector material has a thermalization effect, which combines with the effect of the core; the absence of a breeder blanket allows thermalized neutrons from the shield to re-enter the core. Because the thermal fission cross-sections are up to ~1000 times the fast fission cross-sections, there is the potential for significant power from a relatively small thermal flux. Sensitivity studies[3-11] had shown that any significant thermal power was limited to a small edge region and was masked with a coarse axial flux mesh; an axial flux mesh equivalent to 10 meshes in a half-

height model was adequate to demonstrate the effect, where it was present.

Calculations from the current study were examined for indications of whether there was any significant core edge thermal fission effects. Figure 3.2 shows normalized 70-group flux spectra for the core centre and core edge axial number density meshes, at the central radial mesh, for the reference Pu core condition. There is a difference in thermal neutron fluxes of 2 to 3 orders of magnitude, however, where thermal fission cross-sections are ~1000 times fast cross-sections - the very lowest energy group - the fractional flux is still 2 to 3 orders of magnitude lower than was seen in reference 3-11. However, a plot of unnormalized ratings from the most significant fission isotope, ^{239}Pu, in Figure 3.3 shows a region of significantly enhanced core edge ratings for energy groups 42 to 49 (354 to 48 eV); this is the source of a very small (~1%) increase in core edge mesh rating that could be detected from the axial rating distributions.

There are a number of possible reasons why the results of Figures 3.2 and 3.3 do not show a thermal fission effect to the same degreee as the calculations of reference 3-?. The calculations of reference 3-11 used the JEF2.2[3-12] cross-section library in 25 energy groups (rather than 70 groups); they were for a core including a significant diluent fraction, including some diluent S/As.

A sensitivity study with the same 25 energy group structure as used by JEF showed no significant change. Figures 3.4 and 3.5 show the normalized flux spectra and unnormalized ^{239}Pu fission power distribution for a core with the high quality Pu vector and BeO_2 diluent material: the neutron spectra are not greatly different from the reference case, the additional power from enrgy groups 42 to 49 is of a similar size, however, the total power from above energy group 32 (<2.6 keV) is increased and accounts for ~30% of the total power. The results are typical of those for the various diluent materials.

It is possible that the diluent S/As of reference 3-11 provide a route whereby the flux in the shield, and hence its thermal fraction, is further enhanced. It is also possible that there are

significant differences between JEF and JENDL cross-section data in the thermal region: since the datasets are used for fast reactor calculations, the lower energy thermal groups have not previously been considered to be of the greatest importance.

3.2.2 PERTURBATION ENERGY GROUP ASSESSMENT

The first PERKY calculations were done for a core with high quality Pu, they were calculations with dilution in the form of increased voidage (see Section 5.1). These initial calculations used 18 neutron energy groups, as described in reference 3-1. The $\Delta k/k$ value of Na void worth calculated by PERKY was 0.075%, less than half the value of 0.191% from the difference in k_{eff} between the normal and void states calculated by S-J-C. A number of calculations were undertaken to investigate these results.

Values of $\Delta k/k$ were investigated for both Na void worth and Doppler coefficient. In the original S-J-C calculations the convergence criteria used were 10^{-4} and 10^{-5} for flux and k_{eff} respectively; increasing the accuracy of the S-J-C calculations was investigated by reducing the criteria to 5×10^{-6} and 10^{-6}. In some of the calculations, flux convergence to the tighter criterion was not achieved, though k_{eff} convergence always was. Where appropriate, PERKY perturbation calculations were carried out using 70, rather than 18, energy groups. Both exact and 1'st order perturbation calculations were carried out using PERKY. The results of the various calculations are given in Table 3.4

For the Doppler coefficient all the values given in Table 3.4 were close to one another, within ±2%. For the Na void worth there was a wide variation in $\Delta k/k$ values: changing from 70 to 18 energy groups caused a change of ~30% even for the S-J-C calculations; only when 70 energy groups were used was there a reasonable agreement between the S-J-C and the exact perturbation calculations; there was a very large discrepancy between exact and 1'st order perturbation calculations. It was concluded from this that the calculations for this report should adopt 70 energy groups for the PERKY calculations of Na void components.

Upon further investigation the discrepancy in Na void worths proved explicable. Whilst the S-J-C calculation just took the difference in two k_{eff} values, the PERKY calculations involved the integral summation of a large number of terms (for the 'by isotope' Doppler calculations the number of terms was further increased, since microscopic rather than macroscopic cross-sections were used). It was inevitable that rounding errors in the summation in PERKY would be a source of differences between the two calculated values. The low value of the Na void worth was a consequence of large positive contributions from capture and scattering being very nearly offset by a large negative leakage term. The difference between the 70 group S-J-C value, 0.00145, and the 18 group exact perturbation value, 0.00075, was only ~1% of the total magnitude of all the terms, 0.07242. This was comparable with the differences between PERKY and S-J-C Doppler calculations, where over 90% of the components had the same sign (see Figure 5.6).

Table 3.1 Delayed neutron yield data

Isotope	Delayed Neutron Yield Fraction
^{235}U	0.0167
^{238}U	0.0439
^{238}Pu	0.0079
^{239}Pu	0.0063
^{240}Pu	0.0095
^{241}Pu	0.0152
^{242}Pu	0.0221
^{241}Am	0.0051

Table 3.2 Delayed neutron spectrum data

Neutron Energy Group *	Delayed Neutron Energy Spectrum		
	^{235}U	^{238}U	Pu **
4	0.0201	0.0205	0.0184
5	0.1033	0.0952	0.1021
6	0.3571	0.3506	0.3570
7	0.3273	0.3275	0.3342
8	0.1763	0.1900	0.1692
9	0.0159	0.0162	0.0191

* 18 group spectrum; zero flux in groups 1 to 3, 10 to 18
** Pu spectrum is also used for ^{241}Am

Table 3.3 Effect of axial mesh size (70-group calculations)

No. of Axial Meshes	Keff (EOC)	Reactivity Loss/Cycle (%)	Peak Linear Rating (W/cm)	Na Void (%)	Doppler Constant
coarse Number Density 1 Flux 6	1.03819	4.262	295.4	1.153	-.00549
intermediate Number Density 1 Flux 10	1.03798	4.256	292.0	1.146	-.00546
standard Number Density 4 Flux 10	1.04708	4.304	278.6	1.631	-.00573
fine (flux only) Number Density 4 Flux 20	1.04664	4.310	279.4	1.609	-.00575
fine Number Density 8 Flux 20	1.04711	4.313	278.8	1.608	-.00574

Table 3.4 Perturbation $\Delta k/k$ values for various calculation methods

Calculation Type	Doppler Perturbation		Na Void perturbation	
	70-groups	18-groups	70-groups	18-groups
k_{eff} difference (original accuracy)	-.00167	-.00176	+.00151	+.00191
k_{eff} difference (higher accuracy)	-.00170	-.00170	+.00145	+.00189
exact perturbation	-	-.00170	+.00140	+.00075
1'st order perturbation (by Region)	-	-.00172	-.01382	-.01318
1'st order perturbation (by Isotope)	-	-.00174	-	-

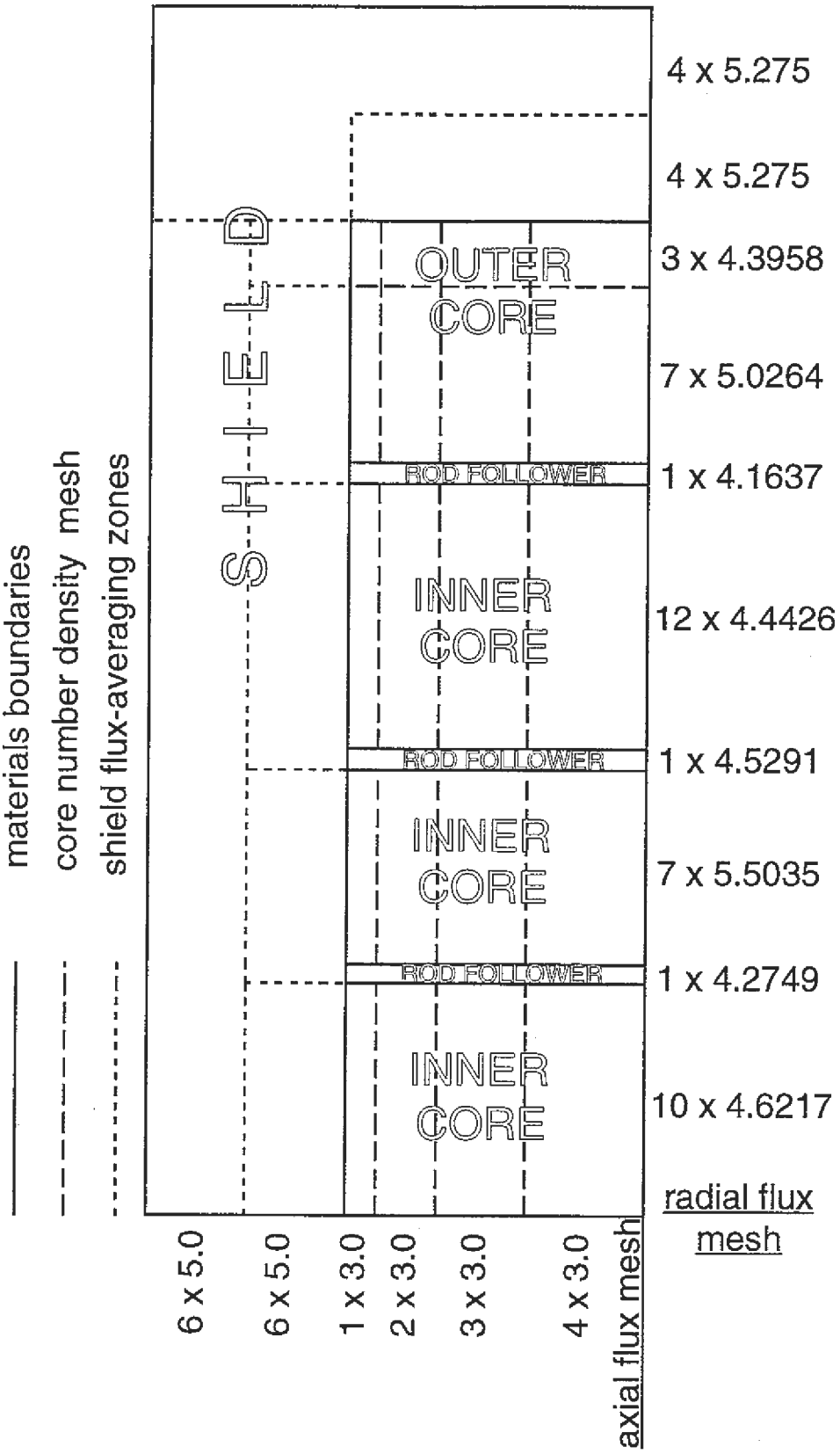

Fig. 3.1 Standard mesh representation

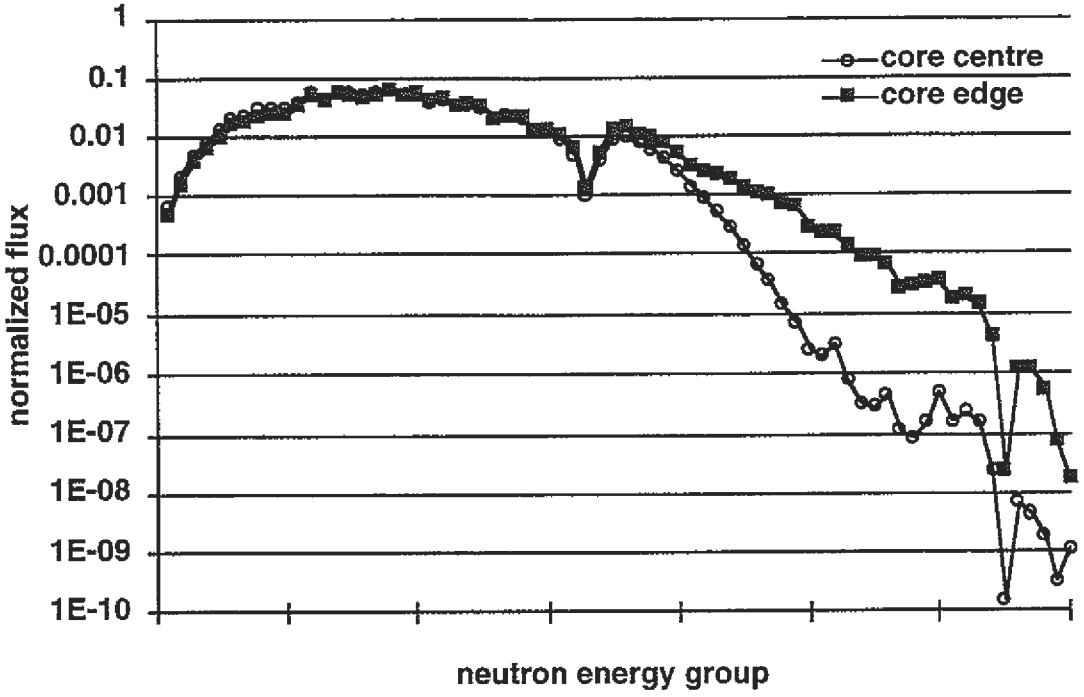

Fig. 3.2 Core edge and core centre neutron energy spectra, reference quality Pu core (no diluent)

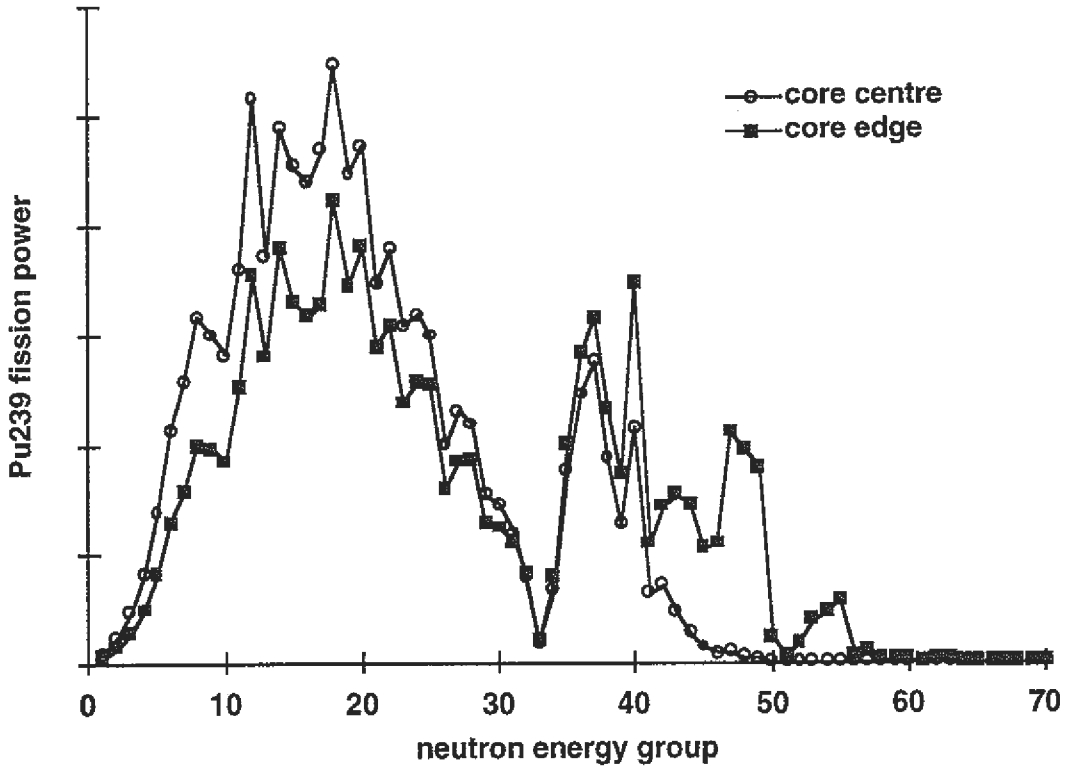

Fig 3.3 Core edge and core centre ^{239}Pu power spectra (unnormalized), reference quality Pu core (no diluent)

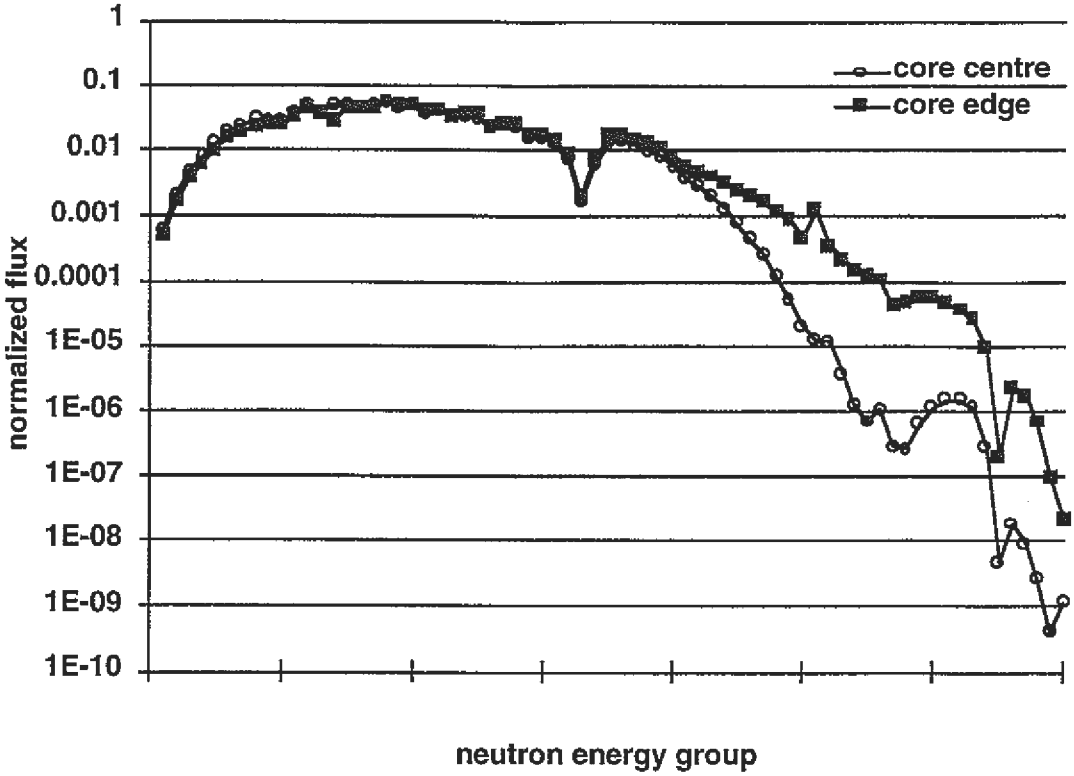

Fig. 3.4 Core edge and core centre neutron energy spectra, high quality Pu core with BeO diluent

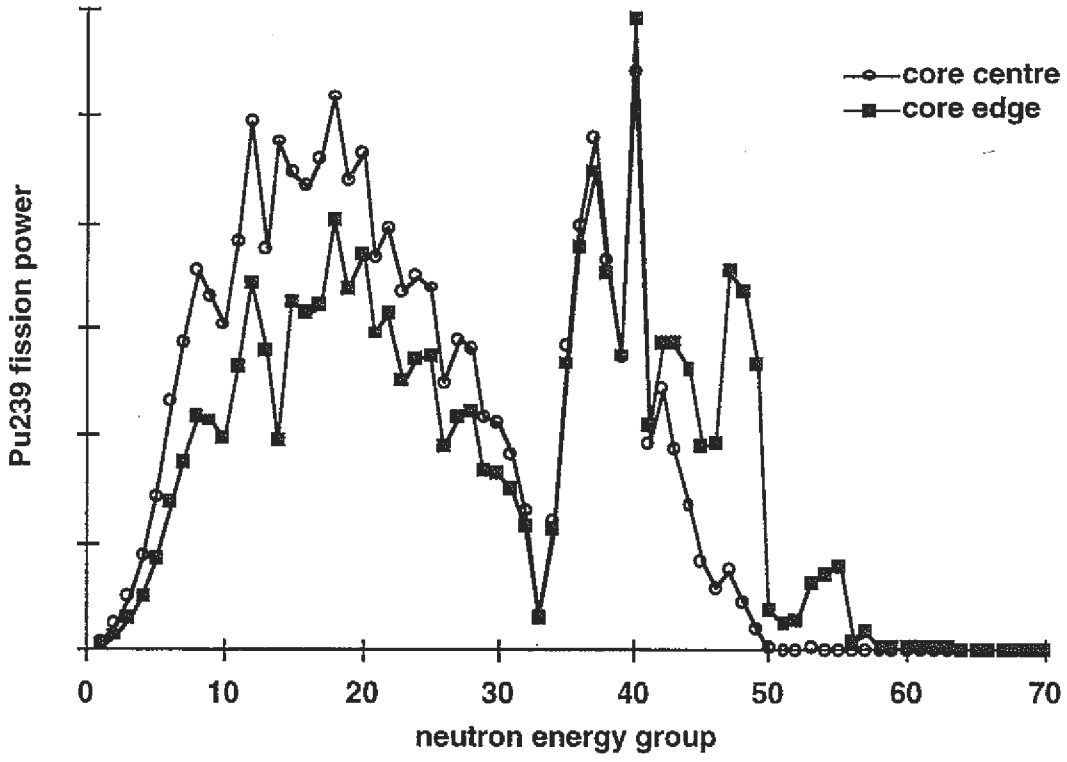

Fig. 3.5 Core edge and core centre ^{239}Pu power spectra (unnormalized), high quality Pu core with BeO diluent

4 REFERENCE QUALITY Pu VECTOR

Reference 1-10 presented a study of cores for the reference quality Pu vector, it produced a design considered to be optimized for Pu burning - that was the design adopted for the current study and described in Chapter 2. In this Chapter, results are presented of calculations that were carried out for the reference Pu vector using the calculational methods described in Chapter 3: they were for the purposes of providing an appropriate reference point against which calculations for the high and low quality Pu vectors could be assessed.

As was noted previously, the calculations of reference 1-10 were for a coarser mesh than was adopted for the current study; it also used older JENDL-2 based cross-section datasets, rather than JENDL-3.2 as in the current study; a different calculational route was used. It was expected that these differences would affect the results of the calculations. Because the reference quality Pu calculation was to be used as a standard against which calculations for high and low quality Pu cores were to be compared, it was important for all the calculations to be on the same basis.

In reference 1-10 the Pu enrichments were 37.5% and 45.0%. It was decided to maintain these values in the current calculations of the reference core. It was considered that the variation in EOEC keff value that was caused would have rather less effect on key parameters than would any changes to Pu enrichments or core design (volume fractions of fuel, steel and Na) that were necessary to re-optimise the core for the current calculational methods.

Table 4.1 shows the results of the reference Pu vector calculations in comparison with the original results from reference 1-10. To investigate the differences in the two calculational routes, calculations were included which used the coarse mesh of reference 1-10, and also using JENDL-2[4-1] based (JFS3-J2) cross-section data.

Table 4.1 shows significant differences between the results from reference 1-10 and those of the calculations done for this report. The effect of axial mesh on Na void worth has already been

addressed in Section 3.2.1, the mesh used in reference 1-10 was a source of significant inaccuracy. The Na void was also sensitive to the choice of cross-section dataset, the later JENDL-3.2 dataset is to be preferred. Relative to the reference 1-10 calculation, the calculations for this report had: keff from 2% to 4 1/2% higher; reactivity loss per cycle ~10% lower; peak rating ~15% lower; Doppler coefficient ~20% larger; neutron lifetime 14% lower and delayed neutron fraction 7% lower. Whilst some of the difference in parameters is a result of mesh and cross-section dataset differences (particularly for Na void, Doppler and k_{eff}), they are generally a result of differences in the calculational routes.

A detailed examination of the calculations for the current report found no significant discrepancies with the calculations of reference 1-10. There were minor differences in core number densities - 0.66% in oxygen and 0.15% in all heavy metal isotopes. PENCIL calculated the pin pitch at 9.48 mm, whilst reference 1-10 quoted 9.65 mm - this was believed to result from a difference in definitions of the term. Neither of these differences is significant.

The reference quality Pu core parameters adopted as a standard for the assessment of high and low quality Pu cores were as follows. A reactivity loss per cycle of 4.304%, Na void worth 1.631%, Doppler coefficient -0.00573, delayed neutron fraction 0.295% and prompt neutron lifetime 0.619×10^{-6} s. These give values of -285 for the void-to-Doppler ratio, -460 and -83 for the secondary safety parameters of void/Doppler.τ and β/Doppler.τ respectively.

A PENCIL calculation was done in which the reference core Pu enrichments were varied, to achieve the reactivity criterion and balanced ratings. The Pu enrichments calculated were 36.44% and 42.64%; The EOEC keff was 1.00513, reactivity loss per cycle 4.64% and peak rating 296 W/cm.

The results for PENCIL and S-J-C in Table 4.1 show variations in peak ratings of a few percent; differences between equivalent PENCIL and S-J-C calculations are reduced from ~5% to ~1% by changing to the finer axial mesh. The variations in k_{eff} showed a systematic difference between the two cross-section datasets, as might be

expected; the difference was ~1%. The difference in k_{eff} for equivalent PENCIL and S-J-C calculations was significantly smaller for the coarse axial mesh, this was considered to have no particular significance. As is shown in Table 4.2, the difference between PENCIL and S-J-C values of k_{eff} can vary significantly with the core composition.

Table 4.3 compares the reference Pu vector, Pu burning core with an equivalent 600 MWe breeder core[1-11]. The Pu burner core shows a significantly larger reactivity loss per cycle, despite the much shorter cycle length, and of course a much higher Pu burning rate. Both Na void worth and Doppler constant are reduced by ~25%, so the void:Doppler ratio is virtually the same.

Table 4.1 Reference Pu core calculations for different calculation routes, cross-sections and meshes

Calculation Type		original calc'n (ref 3-2)	PNC calculation route							
			7 groups	70 groups	7 groups	70 groups	7 groups	70 groups	7 groups	70 groups
No. Density Mesh Size		2 axial 12 rad'l	2 axial 12 rad'l	1 axial 2 rad'l	2 axial 12 rad'l	1 axial 2 rad'l	4 axial, 5 radial		4 axial, 5 radial	
Flux Mesh Size		6 axial	6 axial		6 axial		10 axial		10 axial	
X-Section Dataset		JENDL-2	JENDL-2		JENDL-3.2		JENDL-2		JENDL-3.2	
EOC Keff		-	1.02710	1.03017	1.03707	1.03819	1.04014	1.03767	1.05233	1.04708
Reactivity Loss per Cycle (%)		4.72	4.413	4.335	4.323	4.262	4.337	4.396	4.237	4.304
Peak Linear Rating (W/cm)	BOC (inner)	331	282.8	295.7	282.8	295.4	280.4	283.4	279.9	278.6
	BOC (outer)		270.2	278.8	267.8	275.6	270.2	273.4	267.3	267.7
	EOC (inner)		262.6	280.3	262.8	280.6	261.2	263.4	261.2	259.3
	EOC (outer)		272.7	285.7	270.4	282.3	274.6	278.1	271.1	272.2
Na Void EOC (%) *		1.01	1.530 (1.293)		1.153		1.998		1.631 (1.383)	
Doppler Constant EOC *		-.00429	-.00517 (-.00540)		-.00549		-.00538		-.00573 (-.00588)	
Pu Burn Rate (Kg/TWhe)	(fissile)	76	75.5		74.5		75.6		74.6	
	(all)	75	72.2		72.4		72.1		72.3	
Delayed Neutron Fraction (%)		0.317	-		-		-		0.2954	
Neutron Lifetime (sec x10^{-6})		0.705	-		-		-		0.619	
Safety Comparators	V/D	-235	-296		-210		-371		-285	
	V/(D.τ)	-334							-460	
	β/(D.τ)	-105							-83	
Average Irradiation (GWd/te)		102	102.1		102.1		102.1		102.1	

* values in brackets are BOC

Table 4.2 Discrepancy in k_{eff} between 7 and 70-group calculations

Pu Vector	Non-Standard Conditions	Diluent Material	Keff 7 groups	Keff 70 groups	ΔKeff
reference		-	1.05233	1.04708	-.00525
high quality		void	1.00452	1.00214	-.00238
		MgO	1.00337	1.00206	-.00131
		CeO2	1.00378	1.00203	-.00175
		BeO	1.00618	1.00579	-.00039
		Al2O3	1.00319	1.00146	-.00173
		11B4C	1.00241	1.00145	-.00096
		ZrH1.7	0.99978	1.00411	+.00433
		B4C (92%)	1.00477	1.00146	-.00331
		B4C (30%)	1.00478	0.99952	-.00526
		B4C (5%)	1.00445	0.99864	-.00581
	Pu 45% uniform	B4C (92%)	1.00477	1.00635	+.00158
	Pu 45% uniform	B4C (30%)	1.00481	1.00197	-.00284
		ZrH1.7/B4C	1.00399	1.00399	0.0
low quality	pin size x1.4	ZrH1.7	1.00485	0.99121	-.01364
	pin size x1.8 12 month	ZrH1.7	1.00460	1.01047	+.00587
		11B4C	1.00465	1.00457	-.00008
		BeO	1.00374	1.00326	-.00048
		Al2O3	1.00728	1.00724	-.00004

Table 4.3 Comparison of reference Pu burner core with an equivalent 600 MWe breeder core

	Breeder Core	Burner Core
Core Size, height x diameter (m)	1.0 x 3.0	0.6 x 4.0
Core Volume Fractions (%) (fuel)	42.0	18.0
(coolant)	32.9	64.5
(steel)	22.8	16.3
Fuel Cycle	3 x 15 months	4 x 6 months
Pu % (inner)	17	37.5
(outer)	22	45.0
Na Void (%)	2.2	1.631
Doppler Constant	-.0079	-.00573
Void:Doppler Ratio	-278	-285
Reactivity Loss/Cycle (%)	3.3	4.304
Peak Linear Rating (W/cm)	415	279
Pu Burn Rate (Kg/TWhe) (all)	17	72.3
(fissile)	25	75.3

5 HIGH QUALITY Pu VECTOR

The high quality Pu is more reactive than the reference vector, thus the EOEC reactivity criterion was met for the high quality Pu by reducing the fuel inventory, this was achieved by introducing a diluent material into the core. Several possible diluent materials were assessed.

Initial calculations are presented in Section 5.1, they were done for the simple case of the voidage being increased to replace the removed fuel. The comparative effects of using various materials which are either transparent to neutrons or moderating in nature were examined using a single case from the void-as-diluent calculations, these calculations are presented in Section 5.2. The use of absorber as diluent requires a much lower diluent fraction than do the other options; Section 5.3 presents calculations that were done for absorber as moderator.

The results of the above mentioned calculations showed that using absorber as diluent caused the reactivity loss per cycle to improve (reduce) and the void-to-Doppler ratio safety parameter to worsen (increase in magnitude), relative to the reference quality Pu case. For void, transparent or moderating diluent the opposite occurred: the reactivity loss worsened and the void-to-Doppler ratio improved. In Section 5.4 calculations are presented in which a mixture of absorber and another material are used as diluent, to balance the effects on reactivity loss and safety parameters Section 5.5 presents calculations of the sensitivity to various fuel cycle parameters for a case with a balanced mixture of absorber and moderator as diluent. A summary of the situation for the high quality Pu is given in Section 5.6.

5.1 VOID AS DILUENT

The initial calculations were done with no material replacing the removed fuel. These calculations provided information on the basic core sensitivities, independant of the effects of any diluting material.

The 'type A' pin ratings presented, for dilution within the fuel pellets, could be interpreted as either fuel of a reduced fraction of theoretical density, or as hollow pellets. Table 5.1 shows reduced fractional density and hollow pellet inner diameters corresponding to the range of diluent fractions. The 'type B' pin ratings correspond to the dilution void being in unfuelled, empty, pins,

A series of PENCIL calculations were done for a range of diluent volume fractions, and for fuel cycles of 4, 5 and 6 batches, all for irradiation cycles of 6 months length. Figures 5.1 to 5.3 show how key parameters obtained from PENCIL - peak Pu enrichment, peak pin rating and reactivity loss per cycle - varied with diluent fraction and number of batches.

The only significant variation with the number of batches occurred in peak Pu enrichment; however, since the aim was to define a fuel cycle with a set peak Pu enrichment of 45%, this effectively meant that increasing the number of irradiation batches had the effect of reducing the diluent fraction, and consequently reducing both reactivity loss and type B linear rating. Type A linear ratings (for dilution within the pellet) were only marginally affected by changes in diluent fraction or number of batches.

For each of the number of fuel batches, the fuel fraction that corresponds to a peak Pu enrichment of 45% was obtained by interpolating in Figure 5.1. For these conditions, the complete 'basic' calculation of PENCIL, CITDENS and S-J-C was run, the results of those calculations are given in Table 5.2

Apart from the effects of varying the number of irradiation batches mentioned above, Table 5.2 also shows some significant differences from the reference Pu calculations: both Na void and the void:Doppler ratio are greatly improved, but there is an equally significant degradation in the reactivity loss. The reference quality Pu results are given in Table 5.3.

A variation on the core design was assessed. This had the maximum Pu enrichment of 45% in all the fuel, a balance in peak ratings between the two core zones was achieved by having differential diluent fractions. This variation was examined because

it has the potential to further increase the Pu burning rate. The calculations were done for the same 4 batch irradiation cycle as the reference quality Pu case.

Initial PENCIL sensitivity calculations were done with the diluent fraction in the outer zone fixed at 57 pins - this corresponds to the case of Table 5.2, where this region already had 45% Pu. Figure 5.4 shows the Pu enrichments determined by the PENCIL calculations as a function of the inner zone diluent fraction; Figure 5.5 shows the corresponding inner zone peak linear ratings. The linear rating results of Figure 5.5 imply that the use of a uniform 45% Pu enrichment would only be feasible if the diluent material were incorporated in the fuel pellets; as will be seen in Section 5.5, this is not necessarily so when absorber is used as diluent, because the diluent fraction is lower.

From interpolating in the results of the above PENCIL calculations an optimised core design was found, this consisted of inner and outer zone diluent fractions of 77 and 59 pins respectively. The results of the 'basic' calculation sequence for this optimised condition are given in Table 5.3 - the Pu enrichments are not exactly 45%, this is because the diluent fractions were (arbitrarily) restricted to whole numbers of pins. Table 5.3 includes results for the equivalent case with a uniform diluent fraction (from Table 5.1), and for the reference quality Pu core; it also includes a further variation in which no diluting material was included in the core.

The uniform 45% Pu core showed an increase in Pu burning rate of ~6% compared with equivalent case with uniform fuel fractions. The improvement in Na void noted for the calculations of Table 5.2 was further enhanced to the point where it has a negative value, the degradation in reactivity loss is also increased.

The case where no dilution is used was included to indicate the penalty in terms of Pu burning rate that would be incurred if reduced Pu enrichment, rather than dilution of the core, was used to control the reactivity. It showed Na void and Doppler parameters improved over the reference Pu core, with a comparatively small increase in the reactivity loss. This was achieved with a peak Pu enrichment of

only 34.36%, rather than 45%; the associated reduction in the Pu burning rate was ~25%.

PERKY perturbation calculations were used to produce the neutron lifetime and delayed neutron fraction values for the uniform diluent fraction case in Table 5.3. The results of other perturbations for this core are more appropriately presented in the following section.

A fuel cycle of 4 batches with irradiation cycles of 6 months, a 45% peak Pu enrichment, together with a uniform diluent fraction (rather than a uniform Pu enrichment) have generally been used for the calculations of the following sections. This selection was made mainly on grounds of calculational efficiency, it does not necessarily imply that these are optimal values. The results of the current section can be used to infer the effects of changing the number of batches etc. on later calculations. The effect of varying numbers of batches etc. are again addressed in Section 5.6

In the calculations for the following sections, PENCIL sensitivity calculations as described above have generally been used to define the fuel cycle conditions which are then used in a full 'basic' calculation of PENCIL, CITDENS and S-J-C. However, for reasons of brevity the PENCIL sensitivity calculations are not presented here.

5.2 'TRANSPARENT' AND MODERATING DILUENT MATERIALS

Four separate materials were considered in the role of 'transparent' diluent: MgO, CeO_2, BeO and Al_2O_3. Two different moderator materials have been examined: B_4C in which there is 100% ^{11}B and ZrH with a stochiometry of 1.7. The results showed no sharp difference in the effects of diluents ranging from 'void' to 'transparent' to moderating materials.

Initial calculations with these materials took a case from the 'void' diluent calculations of Section 5.1 and just replaced the 'void' by each of the four 'transparent' and two moderating materials in turn. None of the fuel cycle parameters - Pu enrichment, diluent

fraction etc. - were changed, so these calculations demonstrated the effects that the diluent materials had independant of any changes that would be necessary to re-optimise the fuel cycle.

The calculations were done for a fuel cycle of 4 batches with a cycle length of 6 months, with Pu enrichments of 39.24% and 45.00% for the inner and outer zones respectively, the diluent fraction corresponded to 160 pins of fuel and 57 pins of diluent in each S/A (remembering that the calculations most closely represent the fuel and diluent mixed together in the fuel pellets). For each diluent material, the 'basic' calculation was done and also the PERKY perturbation calculations.

The results are given in Table 5.4, with the PERKY-calculated components of Doppler and Na void shown in Figures 5.6 and 5.7 respectively. The table and figures include results for the 'void' diluent calculations, for ease of comparison.

The four 'transparent' materials were not too different from each other in their effects, with BeO standing out slightly from the others in showing some improvement in the Na void and Doppler parameters, it also showed some difference in k_{eff} values and in the balance between the total and fissile isotope Pu burning rates. All the 'transparent' diluents showed significant improvements in Doppler coefficient (7 to 37%) and in neutron lifetime (2 to 8%), relative to the 'void' diluent case. The superficially large variations in Na void worth, up to 42%, are a consequence of the leakage effect almost balancing the other terms to give values near zero (see Figure 5.7), relative to the reference Pu core, the Na void variation is no more than 4%. The results for $^{11}B_4C$ are similar to those for BeO, indicating that there is no clear demarcation between 'transparent' and moderator materials. The results for $ZrH_{1.7}$ were broadly similar to those of the other diluent materials; the most notable difference occurred in the Doppler constant, which was two to three times the size of values for other materials; also, the neutron lifetime was 24% longer than the next highest value.

The Doppler and Na void components of Figures 5.6 and 5.7 showed the same basic trends for all the diluent materials, though there was a distinct differemce discernable between $ZrH_{1.7}$ and the

other materials. The contribution to Doppler from the structural materials was a comparatively low fraction of the overall effect, from 8% to 23%, the lower value occurring with $ZrH_{1.7}$ diluent; ^{238}U provides nearly all the remainder. The total Na void worth was much smaller than its components, there is a near balancing of negative leakage and fission terms by the positive capture and scattering terms.

The next stage of the assessment was to ascertain the effects of altering the core composition (i.e. diluent fraction and Pu enrichment) in order to re-optimize the EOEC k_{eff} and rating balance for the different diluent materials. Both moderators, 11B4C and ZrH1.7, were included in the calculations, but only two of the 'transparent' materials. From the point of view of fabrication and chemical compatibility, MgO and Al_2O_3 were preferred candidates for 'transparent' diluent materials, Al_2O_3 was selected because it had marginally better Na void and Doppler characteristics. BeO was selected as the second 'transparent' material, because it's behaviour was slightly different from that of the other 'transparent' materials.

A series of PENCIL sensitivity calculations showed that the increases in diluent fractions required were as follows: 1 pin, 3 pins, 1.3 pins and 6 pins, for Al_2O_3, BeO, $^{11}B_4C$ and $ZrH_{1.7}$ diluents respectively. A 'basic' calculation sequence was done for each of these re-optimized core conditions; the results are shown in Table 5.5, with the unoptimised results for comparison.

As was expected given the small changes in diluent fraction, there is generally little change in the results. The most significant change is in the 'type B' pin ratings, they were previously all below 400 W/cm but peak values now approach 430 W/cm. For BeO there is further improvement in the Na void comparable to that already noted; the reactivity loss is increased, by 1 to 5%; for $ZrH_{1.7}$ the Pu burning rate increases 3%.

As was noted in Chapter 4, the differences in k_{eff} between PENCIL (7-group) and S-J-C (70-group) calculations varies significantly with the choice of diluent material. For $ZrH_{1.7}$

diluent there is also a significant discrepancy in the reactivity loss calculated by the two programs.

5.3 ABSORBER ($^{10}B_4C$) AS DILUENT MATERIAL

The final category of diluent material considered was absorber. The only material that has been assessed is B_4C, in which the ^{10}B content has been enriched to 92% (the level in control absorbers) to enhance the absorption. The calculational route does not directly model homogenization effects in absorbers; an attempt to allow for such effects was made by covering a range of ^{10}B fractions in the assessment. It was considered that for B_4C with a given level of ^{10}B incorporated in a core design, there would be some lower ^{10}B fraction which if used in the homogeneous core calculations would give results approximating to the effects of absorber homogenization.

The calculations examined a range of ^{10}B fractions from 92%, the control rod specification, to 30%, a value used in calculations for a 3600 MW core in the CAPRA studies[1-11] of Pu burning cores. It was considered that this range of ^{10}B fractions would encompass a calculation in which absorber was correctly homogenized for B_4C diluent with a 92% ^{10}B content.

Calculations were once again done for a four batch fuel cycle with 6 month irradiation cycles. As well as the usual case of a uniform diluent fraction and 45% peak Pu enrichment, the variant with a uniform 45% Pu enrichment and differential diluent fractions in the two core zones was examined. PENCIL calculations were used to find optimized diluent fractions and Pu enrichments, which were then used in a series of 'basic' calculation sequences. Results for the two studies are given Tables 5.6 and 5.7 respectively.

All the calculations show the same basic characteristics when compared with the reference quality Pu case of Table 5.3: a large degradation in the Na void and Doppler parameters; a significant reduction in the reactivity loss. Peak linear ratings are not significantly increased - the diluent fractions are small, so the 'type B' ratings are not greatly different from those of 'type A'. As the ^{10}B fraction in the B_4C reduces there is some improvement in

Na void/Doppler and some degradation in reactivity loss, but these variations are small relative to the reference Pu values.

5.4 ABSORBER TOGETHER WITH OTHER DILUENT MATERIALS

The results of Section 5.3 for absorber as diluent, with their improved values for Na void and Doppler but degraded reactivity loss, were a mirror image of the situation where the dilution of the fuel was achieved by the use of 'void', 'transparent' or moderating material. It followed that by using a mix of absorber and one of the other diluent materials it should be possible to find a much better balance between the Na void and Doppler parameters on the one hand and the reactivity loss on the other.

The magnitude of absorber homogenization effects, and hence the reduction in ^{10}B level appropriate to modelling the absorber in the current calculations, will depend on the amount of absorber present and on whether it is mixed with other materials or segregated in separate pins. However, it was not expected that, within reasonable limits, the ^{10}B fraction used in the unhomogenized calculations for a mixture of absorber with another diluent would have much effect on the results: suppose a different ^{10}B fraction had been used, it would just have resulted in the optimized condition having different fractions of (unhomogenized) absorber and the other diluting material - the effective amount of ^{10}B would be virtually the same, as would the total diluent fraction. This should not be significant, since it at most involves the exchange of $^{11}B_4C$ for another material with a similar effect.

The first 'combined' diluent material calculations were with B_4C plus 'void' diluent, this being the simplest option to use to examine the trade-off between absorber and the other material. A ^{10}B fraction in the B_4C of 50% was chosen for the calculations; as already argued, the choice of 50% was not considered significant. Calculations were again done for a four batch fuel cycle with 6 month irradiation cycles; the option of a uniform diluent fraction with 45% peak Pu enrichment was used. As previously, 'basic' calculation sequences were performed based on diluent fractions and Pu

enrichments obtained from PENCIL sensitivity calculations. The results are shown in Table 5.8, included are zero B_4C and zero 'void' cases taken from Tables 5.2 and 5.6 respectively.

Using the void-to-Doppler ratio as a comparator, the B_4C fraction would have to be ~3.6 pins or less for this parameter not to exceed the reference quality Pu value. However, at least ~7.4 pins B_4C are required if the reactivity loss is not to exceed that of the reference quality Pu case. (Note that these are not actual fractions of B_4C, since homogenization effects are not directly modelled.) Thus there is no region where both parameters simultaneously achieve the target set by the reference quality Pu case, though the cases with 4 and 6 pins of B_4C come comparatively close.

The next variation considered was to use 'transparent' materials rather than 'void' to mix with the absorber. These calculations were done by repeating one of the calculations of Table 5.8, changing only the materials present - in the same way as the calculations of Table 5.4 relate to one of those in Table 5.2. The case of 6 pins B_4C/32.8 pins 'void' was used; BeO and Al_2O_3 were used as replacement diluent materials; 'basic' calculation sequences were performed for this condition. Table 5.9 shows the results, including the 'void' case for comparison.

The results showed some small improvements in both of the key parameters for BeO; for Al_2O_3 the improvement in reactivity loss is offset by an increase in Na void-to-Doppler ratio. The fuel cycle conditions have not been re-optimized; the results in Table 5.5 indicate that if it were done, then the effects would not be large.

Calculations were then done in which a mix of absorber and moderator were used as the diluent. First of these was to examine $^{11}B_4C$ as moderator: this is easily implimented since it just involves further reducing the ^{10}B fraction below the range covered in Table 5.6, the calculations are otherwise identical. A given fraction of ^{10}B in the (unhomogenized) calculations will correspond to a different (but as yet undefined) ^{10}B fraction in the actual diluent material. This option has the advantage of only involving a single material as diluent, and one which is already validated for in-reactor use. The results are shown in Table 5.10.

For the Na void-to-Doppler ratio not to exceed that for the reference quality Pu, the ^{10}B fraction should be no more than ~3.2%. However, at least ~8.6% ^{10}B is required if the reactivity loss is not to exceed that of the reference quality Pu case. Again there is no region where both parameters are satisfied simultaneously.

Figure 5.8 shows a plot of Na void-to-Doppler ratio versus reactivity loss for the various materials mixed with absorber so far considered. It demonstrates that $^{11}B_4C$ mixed with the absorber produces results that are closest to the target, but there is no great difference between this and other non-absorber diluent materials.

The final variation that was considered was that of $ZrH_{1.7}$ moderator mixed with absorber. It was anticipated that the marked increase in the Doppler parameter associated with this moderator would produce a significant further improvement over the previous calculations. It was decided that this culminating calculation would be done with a uniform Pu enrichment of 45%, since this would maximise the Pu burning rate. It was decided to use a fixed absorber fraction, using only the moderator fraction to balance ratings between the two core zones. Based on the case in Table 5.10 with 10% ^{10}B, an absorber fraction of 3 pins with 92% ^{10}B in the B_4C was chosen. The required target conditions were achieved with $ZrH_{1.7}$ fractions of 52 and 26 pins in the inner and outer core zones respectively. The results are shown in Table 5.11, along with the closest case produced with $^{11}B_4C$ moderator, and the reference quality Pu case, for comparison.

PERKY perturbation calculations were done for the cases of Table 5.11. The components of Doppler and Na void are shown in Figures 5.9 and 5.10. The fraction of the Doppler effect coming from structural materials remains comparatively low. The Na void is still the result of a comparatively small difference in large negative and positive components

It is clear that, with $ZrH_{1.7}$ plus absorber as diluent materials, reactivity loss, Na void, Doppler and all safety parameters can be superior to those in the reference quality Pu case, at the same time the 'type B' linear rating is no more than 376 W/cm.

This is a clear improvement on the case with B_4C as both moderator and absorber, where there remains some small distance from achieving the target values.

5.5 SENSITIVITY TO OTHER PARAMETERS

A number of calculations were done for a core with a combination of absorber and moderator diluent materials, to examine the sensitivity to parameters not varied in Sections 5.2 to 5.4. The calculations were done for a core with B_4C as both moderator and absorber. The results have been used to indicate what changes would be necessary in order for a core with B_4C as both absorber and moderator to achieve the target of parameters no worse than the reference quality Pu case.

The options available to improve the reactivity loss and Na void-to-Doppler combination involve making changes to parameters that may have consequences that are less desirable from an economic standpoint. In particular, a reduced cyle length, reduced number of batches and reduced peak Pu enrichment have been assessed, independantly.

The cases used as a basis for this sensitivity survey were taken from Table 5.10, those having a uniform diluent fraction. PENCIL calculations were used to find optimized values of Pu enrichments and diluent fraction, which were then used in 'basic' calculation sequences. Table 5.12 shows the results for a cycle length reduced to 5 months, Table 5.13 is for 3 batch irradiation and Table 5.14 for a peak Pu enrichment reduced to 40%.

Reducing the cycle length from 6 to 5 months resulted in a range of ^{10}B fractions, from ~4.2% to ~1.8%, where both reactivity loss and Na void-to-Doppler ratio are better than for the reference quality Pu case. Interpolating in these results, a cycle length reduction to ~5.3 months would be sufficient to ensure that the reference quality Pu conditions were achieved.

Reducing the number batches from 4 to 3 resulted in the maximum ^{10}B fraction for an acceptable void-to-Doppler ratio increasing to

~4.1%, whilst the minimum ^{10}B fraction for an acceptable reactivity loss reduces to ~7.4%. Interpolating in the results of Tables 5.12 and 5.13, if the number of irradiation batches were reduced from 4 to 3, then a cycle length of ~5.7 months would be sufficient to ensure that the reference quality Pu conditions were achieved.

Reducing the Pu enrichment from 45% to 40% resulted in ^{10}B fractions greater than ~9.7% producing a reactivity loss less than that of the reference Pu case, whilst less than ~6.0% ^{10}B is necessary for the void-to-Doppler ratio not to exceed that of the reference Pu case. Significant further reduction in Pu enrichment below 40% would be necessary to reduce both parameters to the reference Pu values; such a Pu enrichment would have undesirable consequences on the Pu burning rate.

5.6 SUMMARY

The preceeding sections of this chapter presented calculations that examined the use of different diluent materials in a high quality Pu core, comparing it to an identical core with undiluted reference quality Pu.

The use of increased voidage, a 'transparent' material or moderator as diluent had two main effects relative to the reference quality Pu case. There was a significant improvement in values of Na void and Doppler safety parameters, but also a large degradation (increase) in the rate of reactivity loss. With the diluent material not mixed into the fuel pellets there was also a significant, but acceptable, increase in peak linear ratings. $ZrH_{1.7}$ moderator produced significantly better results than any other material: the Doppler coefficient was 2 to 3 times larger and the neutron lifetime 30 to 40% longer; $^{11}B_4C$ and BeO were both a little better than the remaining diluent materials examined.

A single absorber material was examined, $^{10}B_4C$. The use of absorber as diluent had the effect of reducing the reactivity loss below that of the reference quality Pu core, but degrading the Na void and Doppler parameters; this was the reverse of the results for the other diluent materials. Using absorber as diluent had the

advantage that less diluent was needed, so the effects on peak pin ratings, in the case where diluent was not mixed in the fuel pellet, were smaller than for other materials.

A mixture of absorber together with 'void', 'transparent' or moderator as diluent allowed a balancing of the effects on reactivity loss and on the Na void and Doppler parameters.

A core design variant was considered which adopted differential diluent fractions in the two core zones, allowing a uniform Pu enrichment of 45% to be used. This resulted in ~6% increase in Pu burning rates relative to a core with a uniform diluent fraction. Inner zone peak pin ratings are further enhanced with such a variation, if the diluent is not incorporated within the fuel pellets.

A 'best' core and fuel cycle design was produced, using $ZrH_{1.7}$ moderator mixed with $^{10}B_4C$ absorber as diluent, it incorporated differential diluent fractions and a uniform Pu enrichment of 45%. The targets of reactivity loss and Na void and Doppler related safety parameters no worse than the reference quality Pu core were met (see Table 5.11). The peak pin rating maintains a 12% margin to the limit of 430 W/cm, even when the diluent is separated from the fuel.

Of the other diluent combinations examined, the use of B_4C (i.e. $^{11}B_4C$ as both moderator and $^{10}B_4C$ as absorber) gave marginally the best results. It is not as effective as the $ZrH_{1.7}/^{11}B_4C$ combination, it does not quite achieve the conditions of the reference Pu core (e.g. with the same Na void-to-Doppler ratio the reactivity loss per cycle is ~4.9%, against a target of 4.3%). A relatively small reduction in the irradiation - from four batches of 6 months to four batches of ~5.3 months or three batches of ~5.7 months - would be sufficient to enable the reference Pu core conditions to be achieved.

Subsequent to the calculations for the high quality Pu core presented in Chapter 5, calculations for the low quality Pu core (Chapter 6) exposed a need to modify the standard core design from reference 1-10. The consequences of the modification on the high quality Pu core are addressed in Section 6.4.

Table 5.1 Equivalent diluent fractions for hollow fuel pellets

UO_2 Density (fraction of T.D.)	0.9	0.85	0.8	0.75	0.7	0.65	0.6	0.55
Equivalent Diluent Fraction	0.0	.0556	.1111	.1667	.2222	.2778	.3333	.3889
Equivalent Number of Diluent Pins	0.0	12.1	24.1	36.2	48.2	60.3	72.3	84.4
Hollow Pellet Inner Diameter (mm)	0.0	1.127	1.594	1.952	2.254	2.520	2.760	2.981

(pellet outer diameter is 4.781 mm)

Table 5.2 High quality Pu with 'void' diluent for 4, 5 and 6 batches

No. of Batches		4	5	6	Reference Pu Core
Diluent Fraction (pins)		57	50	43	none
Pu (%)	(inner)	39.24	39.86	40.23	37.5
	(outer)	45.00	45.00	44.88	45.0
Na Void (%)		0.140	0.445	0.710	1.631
Doppler Constant		-.00554	-.00529	-.00509	-.00573
Void:Doppler Ratio		-25	-84	-139	-285
Peak Linear Rating (W/cm)	(type A)	292.6	289.5	286.8	279.9
	(type B)	396.8	376.2	357.7	279.9
Reactivity Loss per Cycle (%)	(70gp)	5.899	5.756	5.619	4.304
	(7gp)	5.879	5.726	5.595	4.237
EOC Keff	(70gp)	1.00214	1.00219	1.00203	1.04708
	(7gp)	1.00452	1.00455	1.00436	1.05233
Pu Burn Rate (Kg/TWhe)	(all)	72.0	71.7	71.7	72.3
	(fissile)	95.5	94.1	93.3	74.6
Average Irradiation (GWd/te)		138.4	165.7	190.8	102.1

Table 5.3 Reference and High quality Pu: various cases for 4 batches

		Reference Pu Core	Uniform 45% Pu Enrichment	Uniform Diluent Fraction	No Diluent
Diluent Fraction (pins)		none	77 / 59	57 / 57	none
Pu (%)	(inner)	37.5	44.92	39.24	29.27
	(outer)	45.0	44.90	45.00	34.36
Na Void (%)		1.631	-0.214	0.140	1.228
Doppler Constant		-.00573	-.00508	-.00554	-.00684
Void:Doppler Ratio		-285	+42	-25	-180
Peak Linear Rating (W/cm)	(type A)	279.9	298.6	292.6	288.6
	(type B)	279.9	462.8	396.8	288.6
Reactivity Loss per Cycle (%)	(70gp)	4.304	6.319	5.899	4.689
	(7gp)	4.237	6.316	5.879	4.663
EOC Keff	(70gp)	1.04708	1.00185	1.00214	1.00447
	(7gp)	1.05233	1.00452	1.00452	1.00471
Pu Burn Rate (Kg/TWhe)	(all)	72.3	75.9	72.0	56.6
	(fissile)	74.6	99.2	95.5	79.8
Neutron Lifetime (sec x 10^{-6})		0.619		0.827	
Delayed Neutron Fraction (%)		0.2954%		0.2447%	
Safety Comparators	V/D.τ	-460		-31	
	β/D.τ	-83		-53	
Average Irradiation (GWd/te)		102.1	149.2	138.4	102.5

Table 5.4 High quality Pu: effect of 'transparent' and moderating diluents for fixed fuel cycle conditions

Diluent Material		'void'	MgO	BeO	CeO_2	Al_2O_3	$^{11}B_4C$	$ZrH_{1.7}$
Na Void (%)		0.140	0.215	0.100	0.239	0.203	0.036	0.233
Doppler Constant		-.00554	-.00637	-.00759	-.00596	-.00629	-.00713	-.01517
Void:Doppler Ratio		-25	-34	-13	-40	-32	-5	-15
Peak (A)	(70gp)	292.0	293.4	293.0	293.1	293.3	292.9	280.0
Linear	(7gp)	292.6	294.7	293.9	293.7	294.0	292.9	280.2
Rating (B)	(70gp)	396.0	397.9	397.4	397.5	397.8	397.2	379.8
(W/cm)	(7gp)	396.8	399.7	398.6	398.3	398.7	397.2	380.0
Reactivity Loss	(70gp)	5.899	5.916	5.916	5.919	5.921	5.924	6.013
per Cycle (%)	(7gp)	5.879	5.916	5.941	5.907	5.919	5.937	6.655
EOC Keff	(70gp)	1.00214	1.00206	1.00579	1.00203	1.00146	1.00145	1.00411
	(7gp)	1.00452	1.00337	1.00618	1.00378	1.00319	1.00241	0.99978
Pu Burn Rate (Kg/TWhe)	(all)	72.0	70.0	68.7	71.0	70.2	69.5	66.0
	(fissile)	95.5	96.0	97.0	95.8	96.0	96.6	97.9
Neutron Lifetime (sec x 10^{-6})		0.827	0.862	0.894	0.844	0.859	0.881	1.106
Delayed Neutron Fraction (%)		0.2447	0.2437	0.2421	0.2433	0.2436	0.2435	0.2517
Safety Comparators	$V/D.\tau$	-31	-39	-15	-48	-38	-6	-14
	$\beta/D.\tau$	-53	-44	-36	-48	-45	-39	-15
Average Irradiation (GWd/te)		138.4	138.4	138.4	138.4	138.4	138.4	138.4

Table 5.5 High quality Pu: effect of optimization on 'transparent' and moderator diluents

Diluent Material	BeO		Al_2O_3		$^{11}B_4C$		$ZrH_{1.7}$	
Type of Case	standard	optimized	standard	optimized	standard	optimized	standard	optimized
Diluent Fraction (pins)	57	60	57	58	57	58.3	57	63
Pu % (inner)	39.24	40.24	39.24	39.82	39.24	40.00	39.24	42.23
(outer)	45.00	44.96	45.00	44.90	45.00	45.00	45.00	44.91
Na Void (%)	0.100	0.048	0.203	0.196	0.036	0.022	0.233	0.230
Doppler Constant	-.00759	-.00758	-.00629	-.00620	-.00713	-.00705	-.01517	-.01486
Void:Doppler Ratio	-13	-6	-32	-32	-5	-3	-15	-15
Peak (A) (70gp)	293.0	302.4	293.3	299.6	292.9	300.0	280.0	305.0
Linear (7gp)	293.9	303.5	294.0	300.6	292.9	300.8	280.2	305.2
Rating (B) (70gp)	397.4	418.0	397.8	408.9	397.2	410.2	379.8	429.8
(W/cm) (7gp)	398.6	419.5	398.7	410.3	397.2	411.3	380.0	430.0
Reactivity Loss (70gp)	5.916	6.083	5.921	5.979	5.924	5.984	6.013	6.316
per Cycle (7gp)	5.941	6.114	5.919	5.973	5.937	5.999	6.655	7.001
(%)								
(70gp)	1.00579	1.00422	1.00146	1.00272	1.00145	1.00370	1.00411	1.00646
EOC Keff (7gp)	1.00618	1.00466	1.00319	1.00453	1.00241	1.00479	0.99978	1.00478
Pu (all)	68.7	69.3	70.2	70.6	69.5	70.0	66.0	68.2
Burn Rate (fissile)	97.0	97.7	96.0	96.3	96.6	97.2	97.9	100.1
(Kg/TWhe)								
average irradiation (GWd/te)	138.4	141.0	138.4	139.2	138.4	139.5	138.4	143.7

Table 5.6 High quality Pu: B_4C absorber diluent (various ^{10}B fractions) with uniform diluent fraction

^{10}B Fraction	92%	70%	50%	30%
diluent fraction (pins)	8.48	10.37	13.20	18.42
Pu % (inner)	38.71	38.67	38.69	38.69
(outer)	45.00	44.99	45.02	45.00
Na Void (%)	3.634	3.534	3.385	3.076
Doppler Constant	-.00150	-.00160	-.00180	-.00210
Void:Doppler Ratio	-2423	-2209	-1881	-1465
Peak (type A) Linear	285.2	284.9	285.4	286.5
Rating (type B) (W/cm)	296.8	299.2	303.9	313.1
Reactivity (70gp) Loss	3.367	3.419	3.494	3.653
per Cycle (7gp) (%)	3.224	3.279	3.364	3.538
(70gp) EOC Keff	1.00146	1.00076	1.00033	0.99952
(7gp)	1.00477	1.00453	1.00466	1.00478
Pu (all) Burn	77.4	77.1	76.8	76.1
Rate (fissile) (Kg/TWhe)	95.1	95.1	95.1	95.2
Average Irradiation (GWd/te)	106.2	107.2	108.7	111.5

Table 5.7 High quality Pu: B_4C absorber diluent (various ^{10}B fractions) with uniform 45% Pu

^{10}B Fraction	92%	70%	50%	30%
Diluent Fraction (pins) (inner/outer)	14.76 7.51	17.80 9.30	22.25 11.88	30.06 16.99
Na Void (%)	4.134	4.031	3.862	3.514
Doppler Constant	-.00080	-.00091	-.00101	-.00127
Void:Doppler Ratio	-5168	-4430	-3824	-2767
Peak Linear Rating (W/cm) (type A)	285.2	266.2	266.8	272.4
Peak Linear Rating (W/cm) (type B)	306.0	290.0	297.3	316.2
Reactivity Loss per Cycle (%) (70gp)	3.127	3.181	3.270	3.453
Reactivity Loss per Cycle (%) (7gp)	3.225	3.011	3.103	3.295
EOC Keff (70gp)	1.00635	1.00545	1.00406	1.00197
EOC Keff (7gp)	1.00477	1.00474	1.00470	1.00481
Pu Burn Rate (Kg/TWhe) (all)	82.5	82.3	81.9	81.1
Pu Burn Rate (Kg/TWhe) (fissile)	99.2	99.3	99.4	99.5
Average Irradiation (GWd/te)	106.2	108.9	110.8	114.6

Table 5.8 High quality Pu: B_4C absorber (50% ^{10}B) plus 'void' diluent

B_4C Fraction		0	4	6	8	10	13.2
'void' Fraction		57	41.18	32.82	24.05	15.0	0
Pu %	(inner)	39.24	38.71	38.63	38.61	38.61	38.69
	(outer)	45.00	45.00	45.00	45.00	45.00	45.02
Na Void (%)		0.140	1.321	1.834	2.340	2.771	3.385
Doppler Constant		-.00554	-.00404	-.00339	-.00281	-.00238	-.00180
Void:Doppler Ratio		-25	-327	-541	-833	-1164	-1881
Peak Linear Rating (W/cm)	(type A)	292.6	289.5	288.5	287.7	286.8	285.4
	(type B)	396.8	365.6	351.4	337.6	324.1	303.9
Reactivity Loss per Cycle (%)	(70gp)	5.899	4.935	4.548	4.207	3.911	3.494
	(7gp)	5.879	4.876	4.483	4.116	3.796	3.364
EOC Keff	(70gp)	1.00214	0.99868	0.99830	0.99862	0.99909	1.00033
	(7gp)	1.00452	1.00491	1.00460	1.00486	1.00486	1.00466
Pu Burn Rate (Kg/TWhe)	(all)	72.0	73.5	74.3	75.0	75.6	76.1
	(fissile)	95.5	94.6	94.7	94.8	94.9	95.2
Average Irradiation (GWd/te)		138.4	128.9	124.3	119.7	115.3	108.7

Table 5.9 High quality Pu: B_4C absorber plus 'transparent' diluent, for fixed fuel cycle conditions

Diluent Material		'void'	BeO	Al_2O_3
Na Void (%)		1.834	1.904	2.030
Doppler Constant		-.00339	-.00385	-.00343
Void:Doppler Ratio		-541	-495	-592
Peak (A)	(70gp)	284.5	283.5	284.5
Linear	(7gp)	288.5	284.9	285.9
Rating (B)	(70gp)	346.5	345.3	346.5
(W/cm)	(7gp)	351.4	347.0	348.2
Reactivity Loss	(70gp)	4.548	4.433	4.483
per Cycle (%)	(7gp)	4.483	4.386	4.416
EOC Keff	(70gp)	0.99830	0.98273	0.98428
	(7gp)	1.00460	0.98419	0.98652
Pu Burn	(all)	74.3	72.3	73.2
Rate (Kg/TWhe)	(fissile)	94.7	95.9	95.3
Average Irradiation (GWd/te)		124.3	124.3	124.3

Table 5.10 High quality Pu: B_4C as both absorber and moderator (^{10}B fractions <30%)

^{10}B Fraction		20%	10%	5%	3%
Diluent Fraction (pins)		23.32	32.77	40.91	46.04
Pu %	(inner)	38.72	38.83	38.97	39.14
	(outer)	45.01	45.02	45.00	44.98
Na Void (%)		2.773	2.150	1.481	1.395
Doppler Constant		-.00245	-.00331	-.00439	-.00506
Void:Doppler Ratio		-1132	-650	-337	-276
Peak Linear Rating (W/cm)	(type A)	287.2	290.0	292.4	294.4
	(type B)	321.8	341.6	360.3	373.7
Reactivity Loss per Cycle (%)	(70gp)	3.820	4.182	4.622	4.945
	(7gp)	3.714	4.117	4.591	4.935
EOC Keff	(70gp)	0.99883	0.99844	0.99864	0.99976
	(7gp)	1.00469	1.00473	1.00445	1.00488
Pu Burn Rate (Kg/TWhe)	(all)	75.4	74.1	75.6	72.1
	(fissile)	95.2	95.4	94.9	95.6
Average Irradiation (GWd/te)		114.3	119.9	125.7	129.5

Table 5.11 High quality Pu: optimised cases with absorber plus moderator

Diluent Material		$^{11}B_4C$ moderator	$ZrH_{1.7}$ moderator	Reference Quality Pu
Type of Case		uniform pins	uniform Pu	
Diluent Fraction (pins)		40.91 B_4C (5% ^{10}B)	3/3 B_4C (92% ^{10}B); 52/26 $ZrH_{1.7}$	(none)
Pu (%)	(inner)	38.97	45.0	37.5
	(outer)	45.00	45.0	45.0
Na Void (%)		1.481	0.885	1.631
Doppler Constant		-.00439	-.00737	-.00573
Void:Doppler Ratio		-337	-120	-285
Peak Linear Rating (W/cm)	(type A)	292.4	280.3	279.9
	(type B)	360.3	375.5	279.9
Reactivity Loss per Cycle (%)	(70gp)	4.622	3.903	4.304
	(7gp)	4.591	4.113	4.237
EOC Keff	(70gp)	0.99864	1.00399	1.04708
	(7gp)	1.00445	1.00399	1.05233
Pu Burn Rate (Kg/TWhe)	(all)	75.6	73.4	72.3
	(fissile)	94.9	104.1	74.6
Neutron Lifetime (sec x 10^{-6})		0.670	0.717	0.619
Delayed Neutron Fraction (%)		0.2429	0.2352	0.2954
Safety Comparators	$V/D.\tau$	-504	-167	-460
	$\beta/D.\tau$	-83	-45	-83
Average Irradiation (GWd/te)		125.7	125.0	102.1

Table 5.12 High quality Pu: B_4C as both absorber and moderator (^{10}B fractions <30%) - cycle length reduced from 6 to 5 months

^{10}B Fraction		20%	10%	5%	3%
Diluent Fraction (pins)		24.86	34.52	43.70	49.43
Pu %	(inner)	38.30	38.30	38.34	38.46
	(outer)	45.00	45.00	44.96	45.00
Na Void (%)		2.867	2.195	1.474	0.995
Doppler Constant		-.00228	-.00320	-.00429	-.00510
Void:Doppler Ratio		-1257	-686	-344	-195
Peak Linear Rating (W/cm)	(type A)	284.0	286.0	288.4	289.6
	(type B)	320.7	340.1	361.1	375.0
Reactivity Loss per Cycle (%)	(70gp)	3.141	3.449	3.835	4.128
	(7gp)	3.046	3.390	3.810	4.117
EOC Keff	(70gp)	0.99932	0.99863	0.99878	0.99995
	(7gp)	1.00481	1.00474	1.00444	1.00482
Pu Burn Rate (Kg/TWhe)	(all)	76.2	74.7	73.4	72.5
	(fissile)	96.4	96.5	96.7	96.9
Average Irradiation (GWd/te)		96.1	101.1	106.5	110.1

Table 5.13 High quality Pu: B_4C as both absorber and moderator (^{10}B fractions <30%) - number of batches reduced from 4 to 3

^{10}B Fraction		20%	10%	5%	3%
Diluent Fraction (pins)		25.40	35.29	44.94	50.75
Pu %	(inner)	38.34	38.36	38.46	38.54
	(outer)	45.00	45.00	45.03	44.99
Na Void (%)		2.962	2.219	1.478	0.980
Doppler Constant		-.00230	-.00316	-.00419	-.00506
Void:Doppler Ratio		-1288	-702	-353	-194
Peak Linear Rating (W/cm)	(type A)	287.4	290.6	293.6	296.3
	(type B)	325.5	329.1	370.3	386.7
Reactivity Loss per Cycle (%)	(70gp)	3.689	4.067	4.528	4.888
	(7gp)	3.586	3.997	4.502	4.886
EOC Keff	(70gp)	0.99979	0.99897	0.99904	1.00005
	(7gp)	1.00484	1.00498	1.00464	1.00485
Pu Burn Rate (Kg/TWhe)	(all)	75.4	74.7	74.7	72.5
	(fissile)	97.1	96.5	96.5	96.9
Average Irradiation (GWd/te)		86.7	91.4	96.5	99.9

Table 5.14 High quality Pu: B_4C as both absorber and moderator (^{10}B fractions <30%) - Pu enrichment reduced from 45% to 40%

^{10}B Fraction		20%	10%	5%	3%
Diluent Fraction (pins)		12.86	18.46	23.95	27.20
Pu %	(inner)	34.12	34.21	34.33	34.37
	(outer)	40.00	40.00	40.00	40.00
Na Void (%)		2.190	1.791	-1.386	1.129
Doppler Constant		-.00390	-.00465	-.00534	-.00587
Void:Doppler Ratio		-562	-385	-260	-192
Peak Linear	(type A)	287.1	289.0	290.2	290.7
Rating (W/cm)	(type B)	305.2	315.9	326.2	332.4
Reactivity Loss	(70gp)	4.092	4.286	4.640	4.839
per Cycle (%)	(7gp)	4.026	4.303	4.600	4.808
EOC Keff	(70gp)	0.99840	0.99875	0.99938	0.99993
	(7gp)	1.00478	1.00479	1.00480	1.00481
Pu Burn	(all)	68.0	67.2	66.3	65.8
Rate (Kg/TWhe)	(fissile)	88.7	88.7	88.7	88.7
Average Irradiation (GWd/te)		108.7	111.8	114.9	116.9

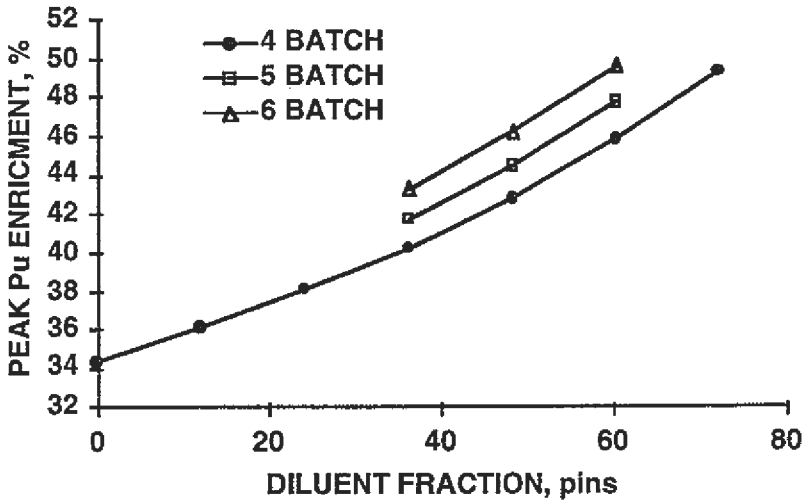

Fig. 5.1 Peak Pu enrichment (%) as a function of diluent fraction and number of irradiation batches

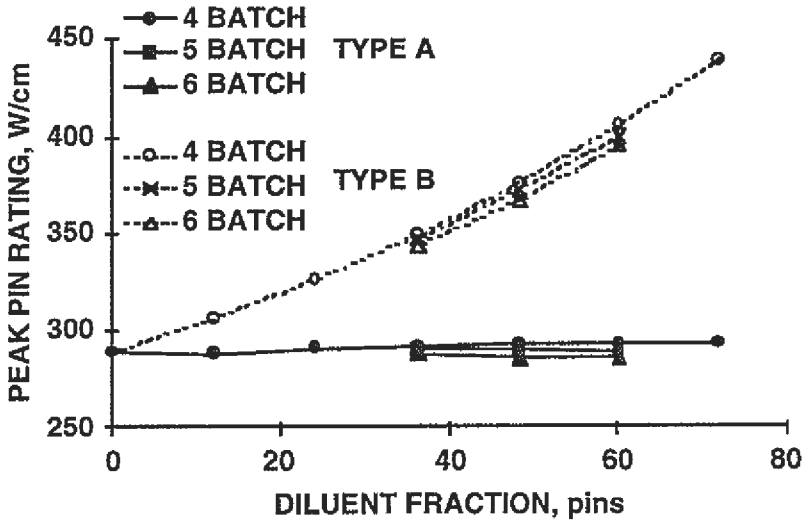

Fig. 5.2 Peak linear rating (W/cm) as a function of diluent fraction and number of irradiation batches

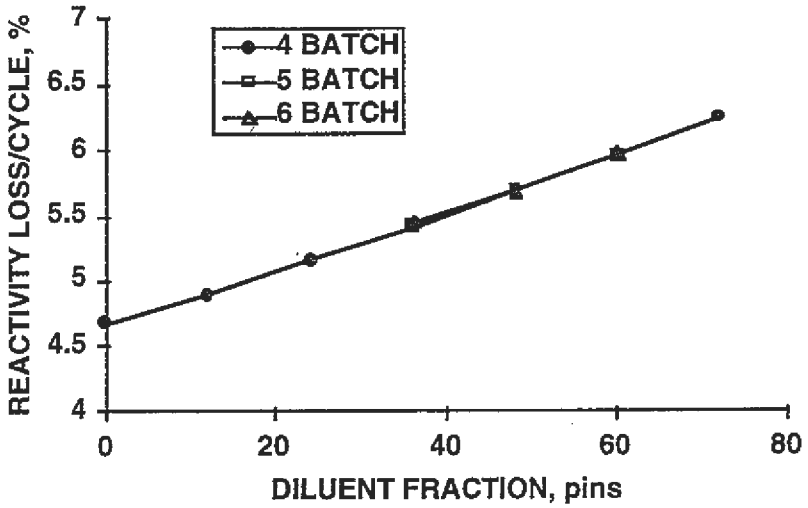

Fig. 5.3 Reactivity loss per cycle (%) as a function of diluent fraction and number of irradiation batches

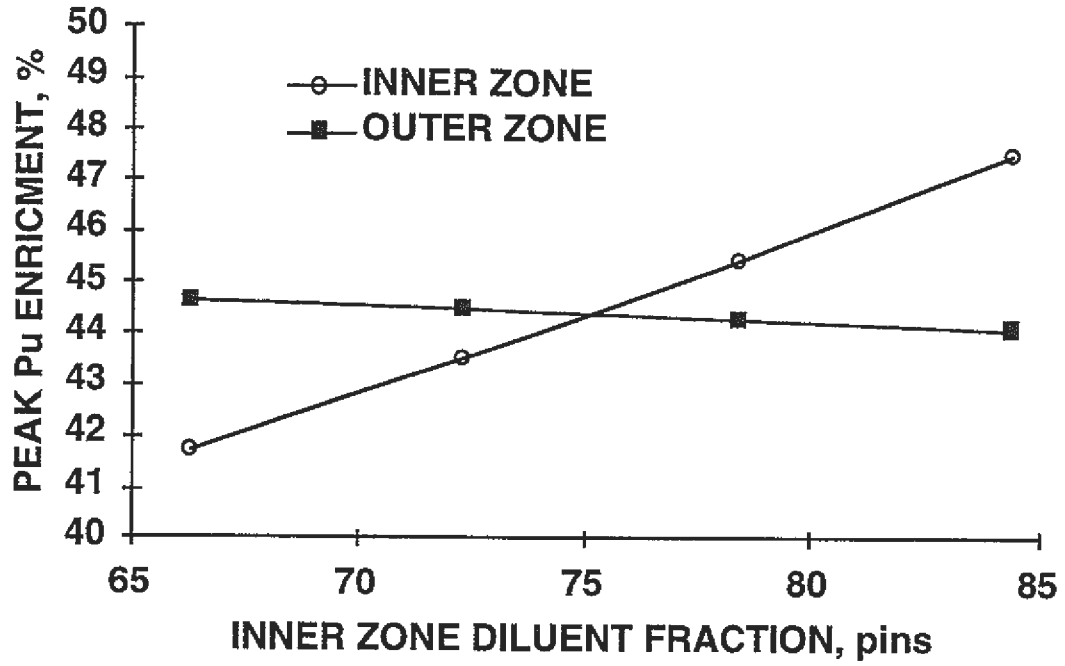

Fig. 5.4 Pu enrichment (%) as a function of inner zone diluent fraction, outer zone diluent fraction fixed at 57 pins

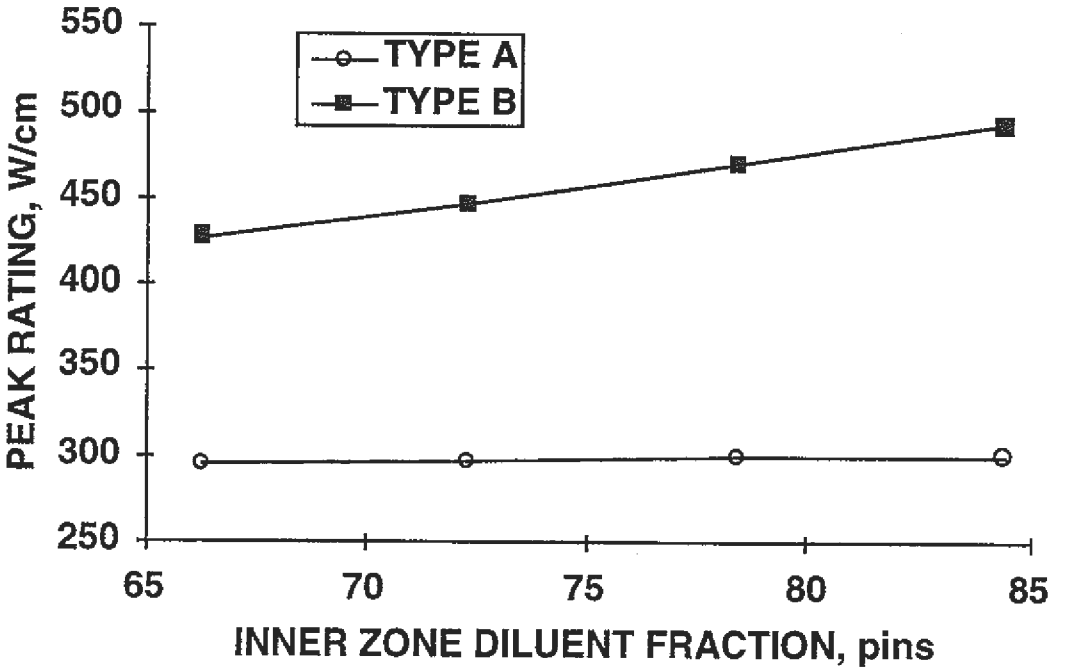

Fig. 5.5 Inner zone peak linear rating (W/cm) as a function of inner zone diluent fraction, outer zone diluent fraction fixed at 57 pins

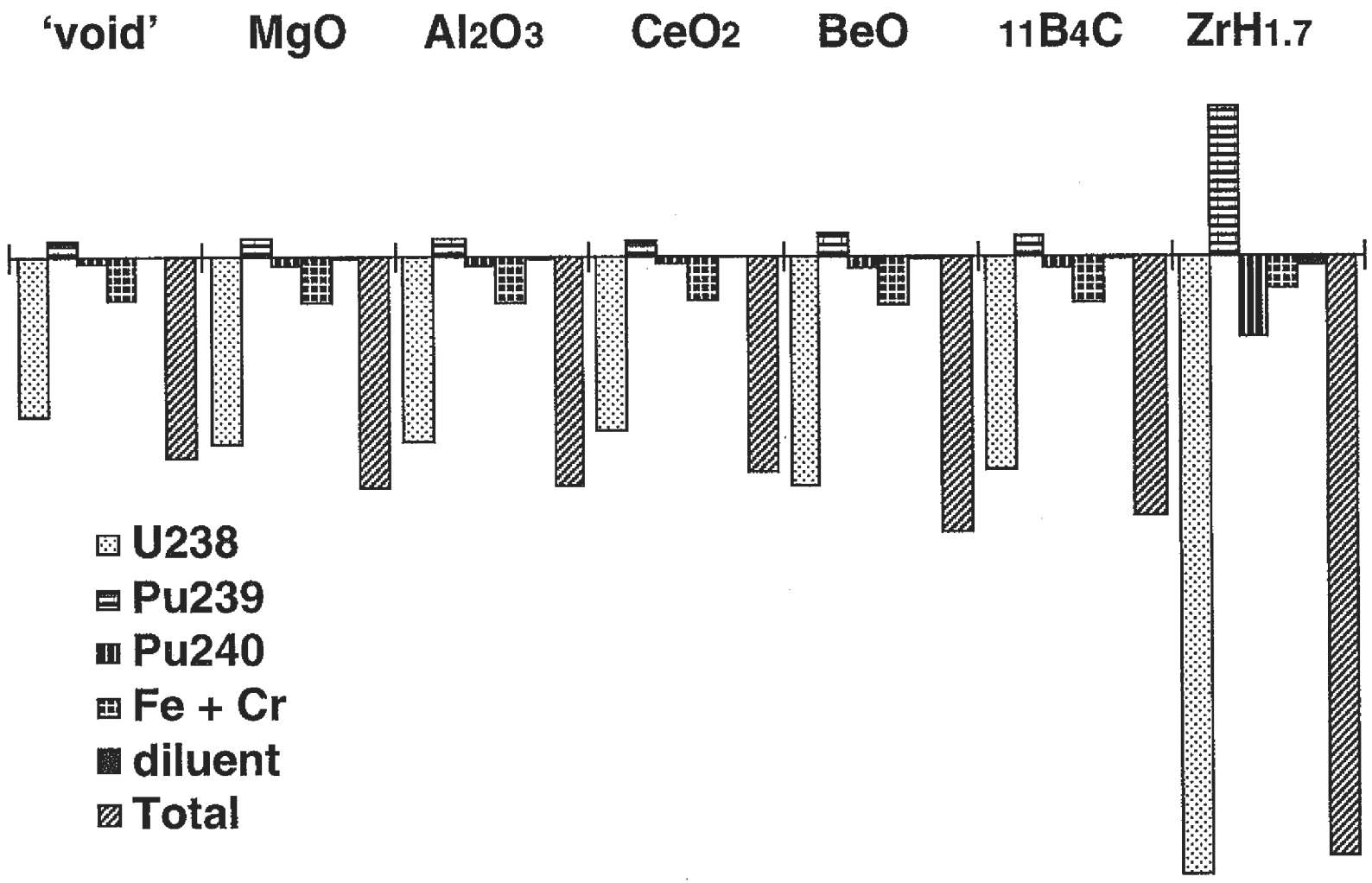

Fig. 5.6 Main Doppler components, high quality Pu with various diluents

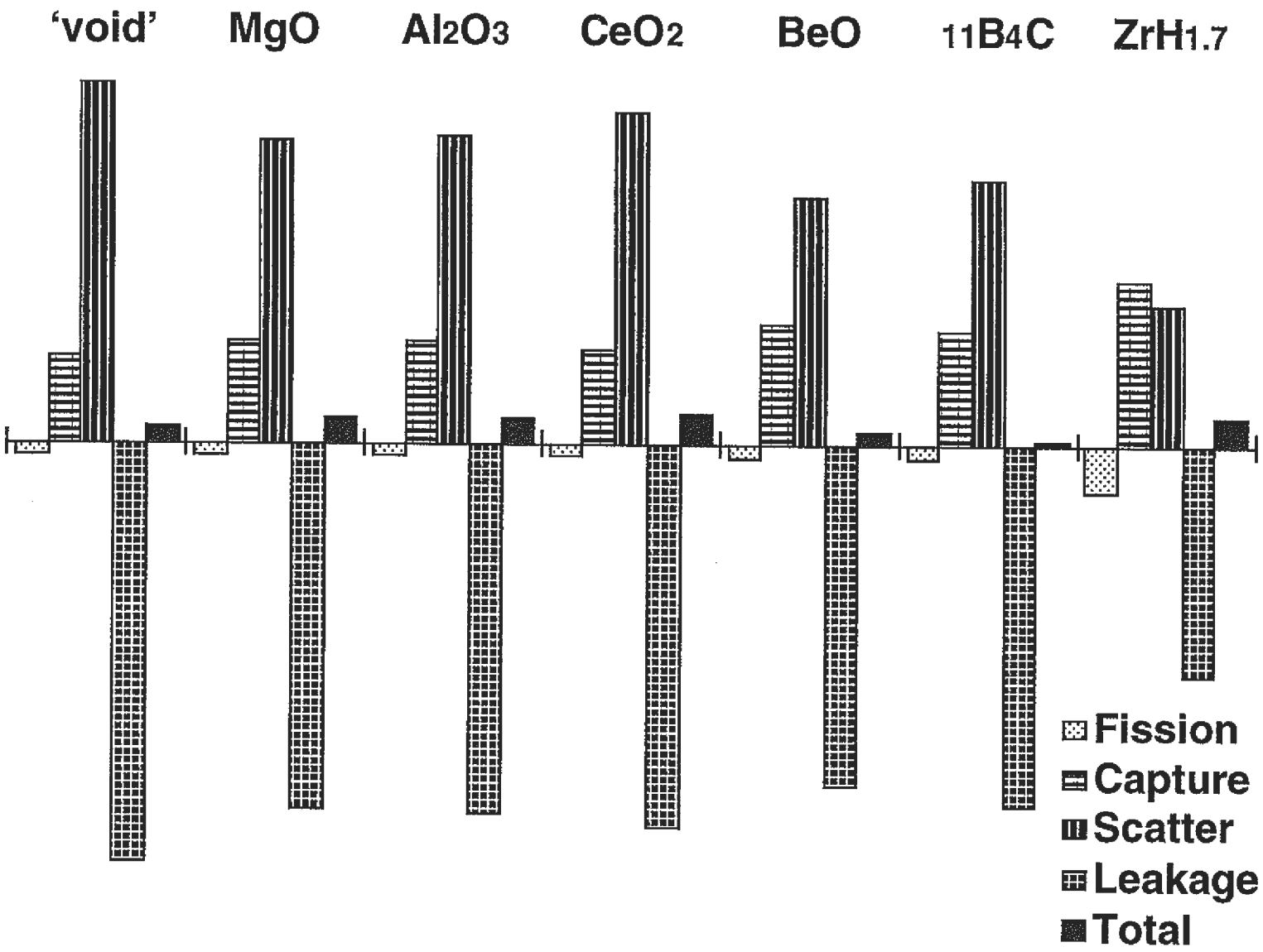

Fig. 5.7 Na void components, high quality Pu with various diluents

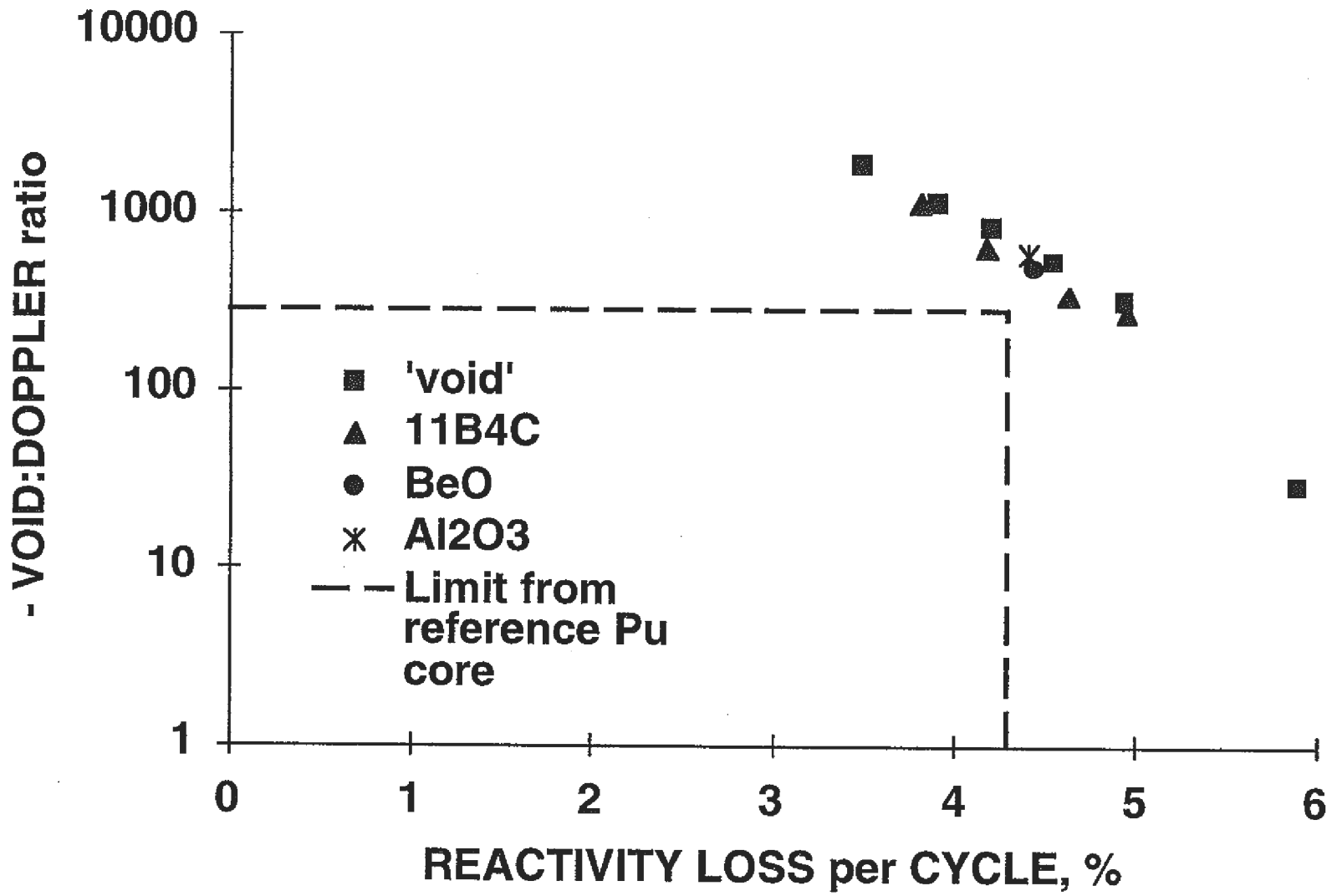

Fig. 5.8 Void:Doppler ratio as a function of reactivity loss per cycle, high quality Pu with diluent of $^{10}B_4C$ plus another material

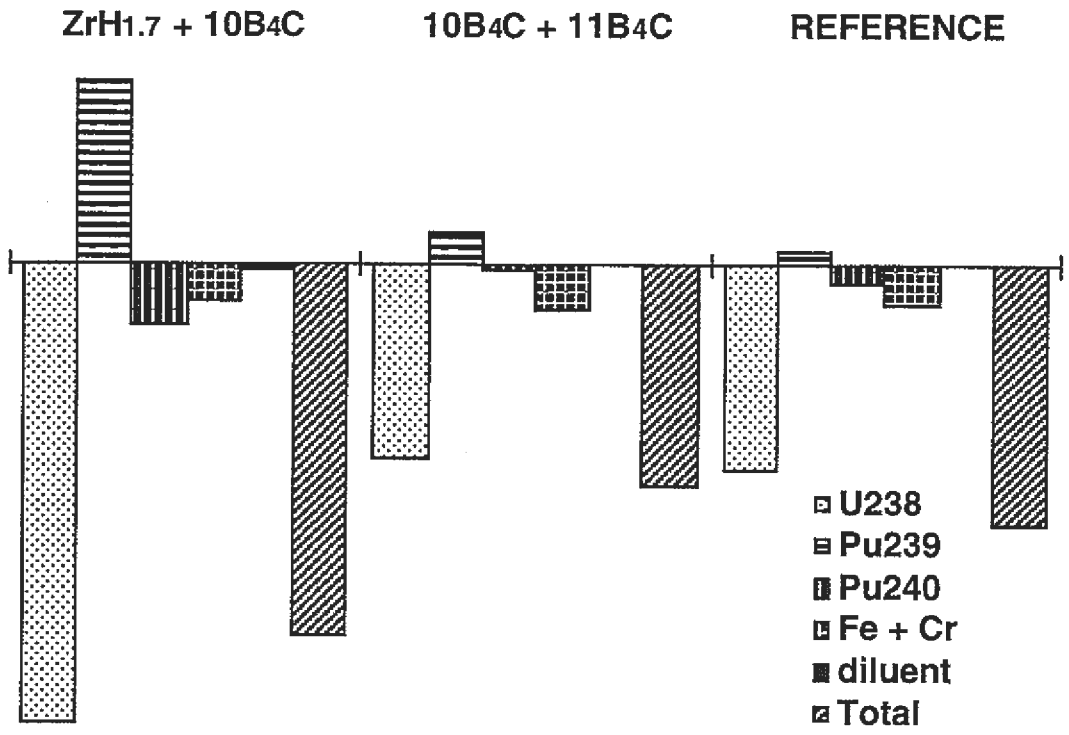

Fig. 5.9 Main Doppler components, high quality Pu with diluent of $^{10}B_4C$ plus another material

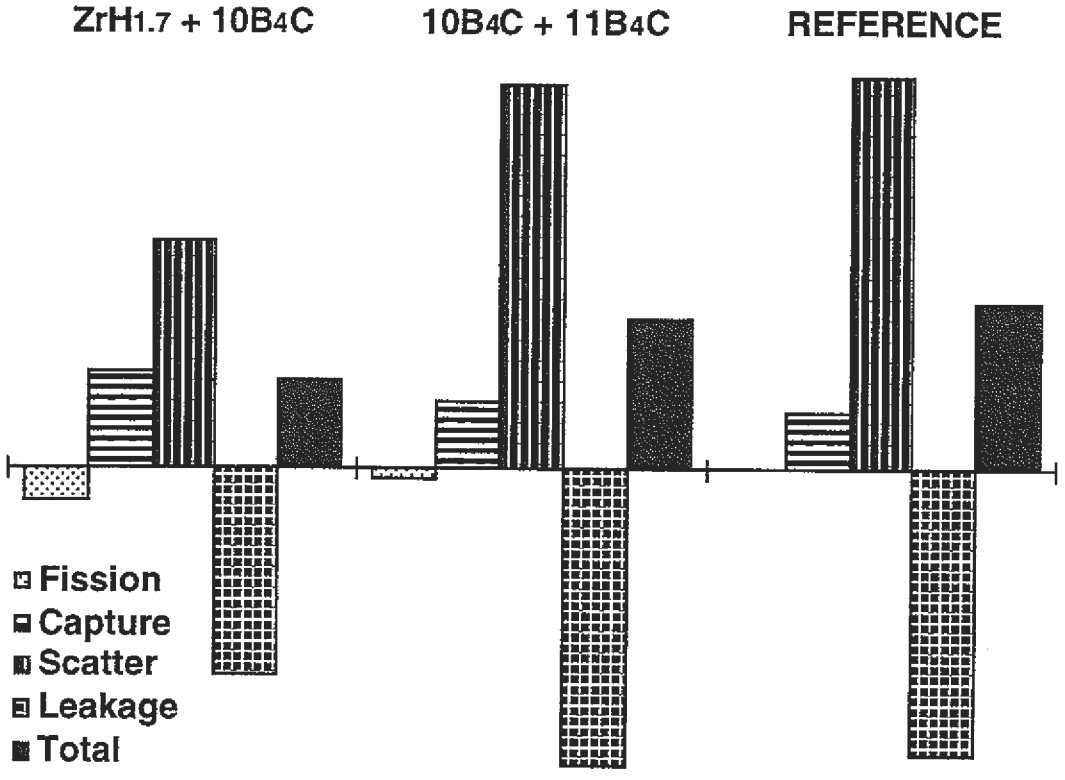

Fig. 5.10 Na void components, high quality Pu with diluent of $^{10}B_4C$ plus another material

6 LOW QUALITY Pu VECTOR

The low quality Pu is less reactive than the reference quality Pu. Section 6.1 presents initial calculations that were done to determine how this might be accommodated within the framework of the reference core design; an increased pin size giving a higher fuel inventory was considered the only practical alternative. An amount of non-absorber diluent material was also considered necessary, to combat a tendency towards degradation of the Na void and Doppler safety parameters.

Section 6.2 presents calculations done with $ZrH_{1.7}$ as diluent, the most effective of those materials examined in the high quality Pu assessment of Chapter 5; a pin volume increased of x1.5 or more was shown to be necessary to match the reference quality Pu core. A number of other diluent materials were addressed in Section 6.3, for those the reference quality Pu conditions were only achieved for a pin volume increase of at least x2.2.

It is inherent in the current study that the same reactor design be assessed for each Pu vector: Section 6.4 presents the results calculations done for the reference and high quality Pu cores but with pin sizes increased by x1.5 and x2.2. The calculations were for B_4C as diluent, the ^{10}B concentration being used to balance the moderator and absorber effects.

6.1 MEASURES TO COUNTER LOW REACTIVITY

In this section calculations are presented that were used to identify whether particular modifications to the fuel cycle or core would enable the low quality Pu fuel to achieve the reactivity target (k_{eff} 1.0048 at EOEC). Given their purpose the calculations, using PENCIL, were generally of a simplified nature: a uniform (45%) Pu enrichment was used, since this would most readily meet the reactivity criterion; at this stage, no 7-group microscopic cross-sections file was produced specifically for the low quality Pu vector.

The initial step was to reduce the fuel irradiation, by reducing the number of fuel batches, leaving the cycle length at 6 months. Table 6.1 shows the results of calculations in which the number of batches was reduced. The EOEC k_{eff} is as low as 0.922 for four batches, reducing to two batches only increases k_{eff} to 0.959.

Table 6.2 shows the results of calculations in which the cycle length was reduced for a 4 batch irradiation cycle. Even with the batch reduced to 4 months the EOEC k_{eff} is only increased to 0.953.

From comparing the k_{eff} of the clean core, 1.021, with the above results, it can be deduced that in order to achieve the required 1.0048 EOEC k_{eff} it would be necessary to reduce the cycle length to 1.5 months or less. Such a short cycle would clearly be impractical from an economic point of view, so it is necessary to look to other measures to increase the core reactivity.

Two possible methods of increasing the core reactivity were identified; both of them suffer from certain drawbacks. The first option was to allow the Pu enrichment to increase above 45%: this is unlikely to be a viable option, because of considerations of fuel solubility during reprocessing. Should higher Pu enrichments become practicable they are likely to be in association with other more radical fuel options, such as 'Pu without U' fuel, which are beyond the scope of the current study. The second alternative was to increase the pin diameter, thus allowing more fuel material to be incorporated in the core. Changing the pin size would compromise the requirement for the same S/A design to be used in the study of all three Pu vectors: although the S/A wrapper remains unaltered, the pin size change would significantly alter the thermo-hydraulic characteristics (e.g. pressure drop) of the S/A. It may be that other modifications to S/A design could be incorporated (e.g. flow restrictors of different sizes) to allow S/As with different pin sizes to have equivalent thermo-hydraulic characteristics, allowing them to be interchangeable within the same reactor design. If such a modification does not prove possible, then it would be necessary to adopt the same enhanced pin size for all Pu vectors

Table 6.3 shows the results of calculations in which the Pu enrichment was increased above 45%. It is seen that enrichments in

the region of 52% would be necessary if that option was used to achieve the required level of criticality.

Table 6.4 presents the results of calculations done to indicate the effect of increasing the size of the fuel pins. For these calculations the amount of fuel was increased by just altering the fuel density (so there was no reduction in Na volume). The results indicated that an increase in the fuel density from 90% of TD to ~107% would be required. This corresponds to an increase in pin diameter from 5.778 mm to ~6.3 mm, altering the pin from 26.28 to ~31.3% of core volume, and consequently reducing the Na volume from 64.46 to ~59.4%. Such a change would be well within the range of Na volume fractions considered when producing the optimized reference Pu core design[1-10].

It was decided that the only option for the low quality Pu core that was viable within the constraints of the current study was to increase the pin size, with the proviso that some re-assessment of both reference and high quality Pu cores would be required using the increased pin size.

At this stage a properly condensed 7-group cross-section dataset was produced for the low quality Pu core and a full 'basic' calculation sequence was done, for a core with a pin size increase of x1.25 (by volume) properly modelled. The results of the calculation are shown in Table 6.5, compared with the reference quality Pu core they showed a greatly reduced rate of reactivity loss but a much increased Na void worth. The results in Chapter 5 showed that the introduction of an amount of non-absorber material as diluent would be effective in producing more acceptable values for the safety parameters - this needs a further increase in pin size above that required for reactivity considerations.

6.2 ZIRCONIUM HYDRIDE MODERATOR AS DILUENT

The calculations in Chapter 5 for the high quality Pu vector demonstrated that, of those examined, the diluent material that was most effective in improving the values of the safety parameters was

$ZrH_{1.7}$. This section presents calculations done for the low quality Pu vector with $ZrH_{1.7}$ diluent.

Calculations were done for a range of enhanced pin sizes, from x1.4 to x1.8 of the original pin volume. The clad thickness to diameter ratio was maintained, giving an unaltered clad hoop stress if pin internal pressure remains unaltered. It was noted that a pin size of up to x2.2 - corresponding to a Na coolant volume of 32.9% - would be within the range of core compositions examined in the optimization of the reference Pu core[1-10].

PENCIL sensitivity calculations were used to ascertain the uniform diluent fraction and Pu enrichments, these were then used in 'basic' sequence calculations. The resulting reactivity losses were low enough to permit calculations for cycle lengths up to 12 months; in all cases 4 batch irradiation was used.

Table 6.6 shows the results of the calculations, with Figure 6.1 showing a plot of the key parameters of reactivity loss per cycle and the void-to-Doppler ratio. Although the Na void worths were typically 2% to 3%, the $ZrH_{1.7}$ caused a sharp increase in the Doppler coefficient, so that for a range of pin sizes and cycle lengths the void-to-Doppler ratio was no worse than for the reference quality Pu core. This was also the case for the rate of reactivity loss.

Two cases that were considered to have achieved the reference Pu target were subject to PERKY perturbation calculations: a near minimum pin size of x1.5, for which the cycle length was 6 months; a maximum cycle length of 12 months, for which the pin size was x1.8 (any larger pin size would permit little further increase in cycle length). Results in Table 6.6 show that the two secondary safety parameters are within the values for the reference quality Pu. The components of the Doppler and Na void parameters are given, along with those for a case from the following section, in Figures 6.2 and 6.3 respectively. In the Doppler coefficient, the contribution from the structural materials remains a comparatively low fraction; however, for the Na void there is a definite change, with the scattering term now dominating other contributions.

A sensitivity calculation was done in which the number of irradiation batches was reduced from 4 to 3. The results are given in Table 6.7. The case used was for a pin size of x1.4 and a 6 month cycle length, the diluent fraction had to be increased from 5 to 8 pins. The reactivity loss per cycle was increased by less than 0.6%. There was an improvement in both Na void worth and Dopler coefficient, sufficient to reduce the void-to-Doppler ratio virtually to the level of the reference quality Pu core.

In all the low quality Pu calculations with $ZrH_{1.7}$ diluent, the highest 'type B' pin rating achieved was 338 W/cm. Even with diluent materials in separate pins, there are good margins to the 430 W/cm pin rating limit.

6.3 OTHER DILUENT MATERIALS

A number of diluent materials other than $ZrH_{1.7}$ were assessed for the low quality Pu core. First $^{11}B_4C$, then BeO and Al_2O_3, were examined, for a single core and fuel cycle condition: x1.6 pin size with a 4 batch, 6 month irradiation cycle.

PENCIL calculations were used to define optimized conditions for the $^{11}B_4C$ diluents, which were then used in a 'basic' calculation. As with the calculations for Section 5.2, the one set of diluent fraction and Pu enrichments (in this case optimized for $^{11}B_4C$) were used in 'basic' calculation sequences for the other diluents. The BeO and Al_2O_3 diluent cases were then re-optimized using PENCIL, and finally the 'basic' sequences were recalculated for the re-optimized condition. The results are shown in Table 6.8, along with the equivalent case with $ZrH_{1.7}$ moderator for comparison.

All four diluent materials show virtually the same reactivity loss, and the re-optimization for BeO and Al_2O_3 required only very minor adjustments to diluent fractions and Pu enrichments. There are significant differences in Na void worth and Doppler coefficient between the four diluents; $ZrH_{1.7}$ is clearly the most effective, with the others following in the order BeO, $^{11}B_4C$, Al_2O_3.

For the Al_2O_3 diluent a series of PENCIL optimization calculations, followed by 'basic' calculation sequences, were done for a range of pin sizes, all for 4 batch irradiation in 6 month cycles. The results are given in Table 6.9; in all cases the reactivity loss per cycle is below 2.5%, but only with a pin size of x2.2 or more does the void-to-Doppler ratio approach that of the reference quality Pu core. PERKY perturbation calculations were done for the x2.2 pin size case; the Doppler and Na void components are in Figures 6.2 and 6.3, they showed similar effects to those noted for $ZrH_{1.7}$ diluent in Section 6.2. Results in Table 6.9 show that the secondary safety parameters fell short of the values for the reference quality Pu core, a consequence of the prompt neutron lifetime being 26% lower.

The pin ratings in Table 6.9 show that, if the diluent is not mixed in the fuel pellet, then the 430 W/cm rating limit will be reached for pin sizes ~x2.2 or larger. The results in Table 6.8 indicate that linear ratings will be very little different if the Al_2O_3 were replaced by BeO, $^{11}B_4C$ or any similar diluent material.

6.4 EFFECTS ON REFERENCE AND HIGH QUALITY Pu VECTOR CASES

The results presented in the previous sections of this chapter demonstrated that, in order to produce an acceptable fuel cycle condition for the low quality Pu vector, it was necessary to increase the pin size and fuel volume fraction above those of the core design optimized[1-10] for reference quality Pu. It remains a central criteria in this study that the S/A designs adopted for the three Pu vectors could be used interchangeably within the same reactor; this may well require the same enhanced pin size to be used for all fuel qualities. This section presents calculations that were done to assess the effects of an increased pin size on the reference and high quality Pu fuel cycles. To attain the criticality target it was, of course, necessary to add some diluent material to the reference quality Pu core and to increase the diluent fraction in the high quality Pu core.

The re-assessment of reference and high quality Pu vectors was done for two separate values of increased pin size: a pin size of x1.5, a minimum value required to make the low quality Pu core viable; a size of x2.2, the level required if the more effective moderating material, $ZrH_{1.7}$, is not used as a diluent in the low quality Pu core. The calculations proceeded as usual - PENCIL sensitivity calculations being used to find optimized core conditions, which were then used in 'basic' calculation sequences. All the cases examined had four batch irradiation with 6 month cycles, the diluent fraction was uniform.

The results of calculations for the reference quality Pu are given in Table 6.10. An initial case was done in which just void was used as diluent: this showed an improvement in Na void and Doppler safety parameters, but an increase in the reactivity loss per cycle. As with the assessment of high quality Pu in Chapter 5, a combination of absorber and another material as diluent was appropriate to restore the balance between the key parameters. Calculations were done in which B_4C was used as both moderator and absorber, several ^{10}B fractions being examined to determine the best balance of absorption and moderation. As the results in Table 6.10 show, ^{10}B fractions were found where B_4C diluent was adequate to produce values of the key parameters that were no worse than those of the reference pin size reference core. With the x2.2 pin size there was some margin to the target values, but for x1.5 pin size the margin was small.

Table 6.11 presents the results of calculations for the high quality Pu core with B_4C as both moderator and absorber. They again demonstrated key parameters meeting targets, with fractionally better margins than for the reference quality Pu calculations of Table 6.10.

The pin ratings in Tables 6.10 and 6.11 showed values that, with the diluent materials segregated from the fuel pellets ('type B'), were above the 430 W/cm limit. For B_4C as diluent, all the cases that met the target reactivity loss and Void-to-Doppler values were above the limit, though for the x1.5 pin size the peak rating might be reduced to ~430 W/cm if the BOEC inner/outer zone ratings were balanced.

It was expected that the adoption of a mixture of $ZrH_{1.7}$ and $^{10}B_4C$ as diluent would both reduce the linear ratings and improve the values of the key parameters. Table 6.12 shows the results of calculations done with a mix of $ZrH_{1.7}$ and $^{10}B_4C$ as diluent, for the high quality Pu with a pin size of x1.5. This diluent option is inappropriate for the x2.2 pin size, since that value only applies if $ZrH_{1.7}$ cannot be used in the low quality Pu core. The high quality Pu case was examined since it produced the highest pin ratings. As Table 6.12 shows, it was possible to produce values of key parameters within targets and at the same time to maintain a 10% margin to the 430 W/cm rating limit.

Should ZrH not prove an acceptable material for diluent, then the x2.2 pin size would be required, producing 'type B' pin ratings of up to 7-800 W/cm for the reference and high quality Pu vectors. For the cases in Tables 6.10 and 6.11, the ratings could be reduced to 430 W/cm by mixing some of the (non-absorber) diluent into the fuel pellets. For the reference quality Pu at least 62 of the 119 pins worth of diluent would have to be incorporated in the fuel pellets. For the high quality Pu case (1.0% ^{10}B) at least 80.5 of the 130.5 pins worth of diluent would have to be incorporated in the fuel pellets. These results should not be very sensitive to the choice of non-absorber diluent material.

6.5 SUMMARY

The calculations for the low quality Pu core concluded that a significant change from the concept of the reference Pu core design was required to achieve the necessary criticality: reducing cycle length to ~1.5 months; increasing Pu enrichment to ~52%; or increasing pin volumes by ~x1.25. Of the three alternatives, only the pin size change was considered viable.

The low quality Pu core demonstrated a reduced reactivity loss, but a degradation in the Na void and Doppler safety parameters, relative to the reference quality Pu core. As was demonstrated for the high quality Pu core in Chapter 5, this can be offset by the

introduction of an amount of non-absorber diluent material. A further pin size increase is necessary to accommodate the diluent.

With $ZrH_{1.7}$ as diluent, the most effective material for improving the Doppler coefficient, it was possible to achieve the reference Pu target values of reactivity loss and safety parameters (see Table 6.6). Various combinations of pin size and cycle length were possible (see Figure 6.1): for a 6 month cycle the pin size could be as low as x1.5; increasing the pin size to x1.8 allowed cycle lengths up to 12 months; further pin size increase would have little effect on cycle length. Reducing the number of batches from 4 to 3 made some improvement in the safety parameters, such that for a 6 month cycle a minimum pin size of x1.4, rather than x1.5, would become acceptable. In all these cases there was a margin of 20% or more to the 430 W/cm rating limit, even for the 'type B' ratings appropriate to fuel and diluent in separate pins.

With another more typical diluent material, Al_2O_3, it was only possible to achieve the target reactivity loss and void-to-Doppler ratio with a pin size of x2.2 and a 6 month cycle length. This produced 'type B' peak pin ratings at the 430 W/cm limit; the secondary safety parameters did not quite achieve the target values. A change to a slightly better diluent material ($^{11}B_4C$ or BeO) and/or a reduction from 4 to 3 batches should be sufficient to bring all parameters within targets, possibly also allowing a slightly longer cycle.

It was required that the S/A designs for the 3 dfferent Pu vectors be interchangeable within the same reactor; it is possible that to meet this criterion the same pin size would have to be used for all Pu vectors. Therefore it was necessary to re-assess the reference and high quality Pu cores with the pin size increased. With the increased pin size, a mix of absorber and moderator diluent was necessary for both reference and high quality Pu core.

Provided that it is acceptable to use $ZrH_{1.7}$ diluent in the low quality Pu core, then a pin size of x1.5 would be adequate. With a x1.5 pin size, a diluent of B_4C (as both moderator and absorber) allowed the reactivity loss and void-to-Doppler ratio to achieve the targets. However, the 'type B' (diluent in separate pins) ratings

were either around (reference quality Pu) or well above (high quality Pu) the 430 W/cm limit. Adopting a mixture of $ZrH_{1.7}$ and $^{11}B_4C$ as diluent both improved the reactivity loss and void-to-Doppler values and also reduced pin ratings so that there was a 10% margin to the 430 W/cm limit.

Without $ZrH_{1.7}$ available as diluent, a pin size of x2.2 would be necessary. Target values of reactivity loss and void-to-Doppler ratio were achieved; however, in order to obtain pin ratings below the 430 W/cm limit a substantial proportion, at least 62%, of the diluent would have to be incorporated in the fuel pellet. These results were reached with B_4C as both moderator and absorber, though there would be no significant difference if any of the other non-absorber diluents were used.

Table 6.1 Low quality Pu: sensitivity to number of irradiation batches (uniform 45% Pu enrichment)

No. of Batches	4	3	2
EOC K-effective	0.92207	0.94040	0.95928
Reactivity Loss per Cycle (%)	4.286	4.234	4.202
Average Irradiation (GWd/te)	101.9	76.4	50.9

Table 6.2 Low quality Pu: sensitivity to cycle length (uniform 45% Pu enrichment)

Cycle Length	6 months	5 months	4 months
EOC K-effective	0.92207	0.93725	0.95275
Reactivity Loss per Cycle (%)	4.286	3.539	2.830
Average Irradiation (GWd/te)	101.9	84.9	67.9

Table 6.3 Low quality Pu: sensitivity to (uniform) Pu enrichment variation

Pu Enrichment (Uniform) (%)	45.0	50.0	55.0
EOC K-effective	0.92207	0.97817	1.03299
Clean Core K-effective	1.02086	1.08390	1.14297
reactivity loss per cycle (%)	4.286	4.091	3.832
average irradiation (GWd/te)	101.9	101.6	101.4

Table 6.4 Low quality Pu: sensitivity to increased fuel density (uniform 45% Pu enrichment)

Fraction of Theoretical Density	0.9	1.0	1.1	1.2
EOC K-effective	0.92207	0.97377	1.02050	1.06301
Reactivity Loss per Cycle (%)	4.286	3.664	3.197	2.827
Average Irradiation (GWd/te)	101.9	91.7	83.3	76.4

Table 6.5 Low quality Pu: pin size x1.25, no diluent

Type of Calculation	Low Quality Pu x1.25 pin size	Reference Pu (for comparison)
Pu % (inner)	40.44	37.50
(outer)	48.62	45.00
Na void (%)	3.568	1.631
Doppler Constant	-.00540	-.00573
Void:Doppler Ratio	-660	-285
Peak Linear Rating (type A) (W/cm)	278.6	279.9
(type B)	278.6	279.9
Reactivity Loss per Cycle (%) (70gp)	2.868	4.304
(7gp)	2.812	4.237
EOC Keff (70gp)	1.00059	1.04708
(7gp)	1.00202	1.05233
Pu Burn Rate (all) (Kg/TWhe)	72.7	72.3
(fissile)	37.7	74.6
Average Irradiation (GWd/te)	81.5	102.1

Table 6.6 Low quality Pu: $ZrH_{1.7}$ diluent, various pin sizes and cycle lengths

Pin Size		x1.4		x1.5	x1.6			x1.8			
Na Volume (%)		53.93		51.31	48.68			43.42			
Cycle (months)		6	8	6	6	8	10	6	8	10	12
Diluent Fraction (pins)		5	1	12	19	14	10	33	26	22	18
Pu (%)	(inner)	37.47	37.37	38.07	38.58	38.57	38.60	39.80	39.56	39.99	40.10
	(outer)	44.83	44.86	44.89	44.96	44.89	44.92	45.23	44.87	45.02	45.02
Na Void (%)		3.147	3.536	2.708	2.366	2.602	2.838	1.853	2.036	2.181	2.342
Doppler Constant		-.00822	-.00589	-.01167	-.01440	-.01184	-.00972	-.01929	-.01635	-.01434	-.01244
Void:Doppler Ratio		-383	-601	-232	-164	-220	-292	-96	-125	-152	-188
Peak Linear Rating (W/cm)	(type A)	280.1	279.9	282.7	282.9	284.8	285.7	287.1	290.1	294.7	295.8
	(type B)	286.7	281.2	299.3	310.0	304.4	299.5	338.6	329.6	328.0	322.6
Reactivity Loss per Cycle (%)	(70gp)	2.600	3.454	2.495	2.449	3.147	3.854	2.486	3.074	3.717	4.326
	(7gp)	2.488	3.264	2.435	2.406	3.087	3.756	2.450	3.054	3.701	4.292
EOC Keff	(70gp)	0.99121	0.98299	1.00222	1.00902	1.00494	0.99987	1.01392	1.01441	1.01318	1.01047
	(7gp)	1.00485	1.00485	1.00508	1.00475	1.00477	1.00466	1.00441	1.00472	1.00480	1.00460
Pu Burn Rate (Kg/TWhe)	(all)	67.0	67.3	66.1	65.7	65.6	65.8	66.3	65.6	65.9	65.9
	(fissile)	32.8	32.6	32.9	33.3	32.7	32.4	35.4	33.9	33.7	33.2
Neutron Lifetime (sec x 10^{-6})				0.521							0.443
Delayed Neutron Fraction (%)				0.3183							0.3148
Safety Comparators	V/D.τ			-445							-425
	β/D.τ			-52							-57
Average Irradiation (GWd/te)		74.6	97.6	72.0	69.9	90.9	111.4	66.8	85.8	105.1	123.6

Table 6.7 Low quality Pu: pin size x1.4, $ZrH_{1.7}$ diluent, 6 month cycle, varying numbers of batches

Pin Size	x1.4	
Na Volume (%)	53.93	
Cycle (months)	6	
Number of Batches	4	3
Diluent Fraction (pins)	5	8
Pu (%) (inner) (outer)	37.47 44.83	37.58 44.89
Na Void (%)	3.147	2.917
Doppler Constant	-.00822	-.00992
Void:Doppler Ratio	-383	-294
Peak Linear Rating (W/cm) (type A) (type B)	280.1 286.7	281.0 291.8
Reactivity Loss per Cycle (%) (70gp) (7gp)	2.600 2.488	2.615 2.523
EOC Keff (70gp) (7gp)	0.99121 1.00485	0.99602 1.00473
Pu Burn Rate (Kg/TWhe) (all) (fissile)	67.0 32.8	66.7 33.1
Average Irradiation (GWd/te)	74.6	56.8

Table 6.8 Low quality Pu: pin size x1.6, 6 month cycle, various diluents

Diluent Material		$ZrH_{1.7}$	$^{11}B_4C$	BeO		Al_2O_3	
Type of Case				standard	optimized	standard	optimized
Diluent Fraction (pins)		19	26.7	26.7	26.3	26.7	27.2
Pu (%)	(inner)	38.58	37.90	37.90	37.92	37.90	37.80
	(outer)	44.96	45.00	45.00	44.98	45.00	45.00
Na Void (%)		2.366	2.944	2.853	2.858	3.038	3.037
Doppler Constant		-.01440	-.00650	-.00686	-.00683	-.00592	-.00594
Void:Doppler Ratio		-164	-453	-416	-418	-513	-511
Peak Linear Rating (W/cm)	(type A)	282.9	282.9	281.9	281.9	283.9	282.1
	(type B)	310.0	322.6	321.5	320.8	323.7	322.5
Reactivity Loss per Cycle (%)	(70gp)	2.449	2.468	2.458	2.452	2.473	2.479
	(7gp)	2.406	2.430	2.414	2.404	2.431	2.437
EOC Keff	(70gp)	1.00902	1.00457	1.00326	1.00443	1.00724	1.00505
	(7gp)	1.00475	1.00465	1.00374	1.00490	1.00728	1.00507
Pu Burn Rate (Kg/TWhe)	(all)	65.7	67.0	66.5	66.5	67.4	67.2
	(fissile)	33.3	32.9	32.6	32.6	33.2	33.0
Average Irradiation (GWd/te)		69.9	72.7	72.7	72.6	72.7	72.9

Table 6.9 Low quality Pu: Al_2O_3 diluent, 6 month cycle, various pin sizes

Pin Size		x1.8	x2.0	x2.2
Na Volume (%)		43.42	38.17	32.91
Diluent Fraction (pins)		45.4	60.1	72.1
Pu (%)	(inner)	38.10	38.42	38.71
	(outer)	45.00	44.99	45.01
Na Void (%)		2.665	2.312	1.974
Doppler Constant		-.00621	-.00646	-.00663
Void:Doppler Ratio		-429	-358	-298
Inner/Outer (A)	(BOC)	283.3/283.4	284.4/285.7	285.7/287.8
Peak linear	(EOC)	281.1/281.5	283.6/283.3	285.4/285.3
Ratings (B)	(BOC)	358.3/358.4	393.3/395.1	427.9/431.0
(W/cm)	(EOC)	355.5/356.0	392.2/391.8	427.4/427.3
Reactivity Loss per Cycle (%)	(70gp)	2.414	2.359	2.310
	(7gp)	2.388	2.333	2.306
EOC Keff	(70gp)	1.00787	1.01034	1.01259
	(7gp)	1.00496	1.00496	1.00483
Pu Burn Rate (Kg/TWhe)	(all)	66.9	66.6	66.4
	(fissile)	32.8	32.6	32.5
Neutron Lifetime (sec x 10^{-6})				0.458
Delayed Neutron Fraction (%)				0.3152
Safety Comparators	V/D.τ			-650
	β/D.τ			-104
Average Irradiation (GWd/te)		71.7	70.6	69.5

Table 6.10 Reference quality Pu: various increased pin sizes and diluents, 6 month cycle

^{10}B Fraction		-	5%	3%	1%	0.4%
Pin Size		x1.5				x2.2
Diluent Material		'void'	B_4C			B_4C
Diluent Fraction (pins)		84.6	56.5	65.0	76.4	119
Pu (%)	(inner)	38.52	39.30	39.39	39.49	40.71
	(outer)	44.91	44.79	45.01	44.96	44.88
Na Void (%)		1.270	2.511	2.114	1.470	0.856
Doppler Constant		-.00557	-.00388	-.00492	-.00694	-.00959
Void:Doppler Ratio		-228	-648	-430	-212	-89
Inner/Outer (A)	(BOC)	291.4/259.2	296.6/269.4	296.6/269.1	301.4/266.0	316.8/269.1
Peak Linear	(EOC)	266.9/265.6	279.4/272.8	277.2/273.1	274.0/272.5	278.0/279.0
Ratings (B)	(BOC)	477.6/424.8	401.0/364.2	423.4/384.2	465.2/410.5	701.5/595.9
(W/cm)	(EOC)	437.4/435.3	377.8/368.8	395.7/389.9	422.9/420.6	615.6/617.8
Reactivity Loss	(70gp)	5.022	3.245	3.593	4.311	4.270
per Cycle (%)	(7gp)	4.956	3.135	3.529	4.283	4.305
EOC Keff	(70gp)	1.00011	1.00602	1.00310	1.00280	1.00685
	(7gp)	1.00484	1.00759	1.00509	1.00444	1.00468
Pu Burn	(all)	72.2	74.6	73.2	70.8	69.3
Rate (Kg/TWhe)	(fissile)	74.4	76.8	76.5	75.7	77.6
Average Irradiation (GWd/te)		111.5	91.9	97.1	104.9	102.7

Table 6.11 High quality Pu: various increased pin sizes, B_4C diluent as both moderator and absorber, 6 month cycle

Diluent Material	B_4C					B_4C	
Pin Size	x1.5					x2.2	
^{10}B Fraction (%)	20	10	5	3	2	1	0.8
Diluent Fraction (pins)	47.0	63.5	78.0	87.3	93.1	130.5	133.0
Pu (%) (inner)	39.29	39.61	39.54	39.70	39.78	41.23	41.39
(outer)	44.53	45.06	45.00	45.01	44.84	45.00	45.01
Na Void (%)	3.605	3.054	2.299	1.719	1.307	0.718%	0.610%
Doppler Constant	-.00082	-.00155	-.00288	-.00414	-.00522	-.00709	-.00782
Void:Doppler Ratio	-4395	-1973	-798	-415	-250	-101	-78
Inner/Outer (A) (BOC)	287.9/274.8	289.6/273.3	293.9/270.4	298.3/268.0	302.6/265.4	319.4/268.3	321.3/266.9
Peak Linear (EOC)	276.2/276.2	275.3/275.6	274.7/274.4	273.8/273.5	272.6/272.8	278.1/278.4	278.4/278.3
Ratings (B) (BOC)	367.5/350.8	409.4/386.4	458.8/422.1	499.1/448.4	530.0/464.8	801.3/673.1	830.0/689.5
(W/cm) (EOC)	352.6/352.6	389.2/389.6	428.8/428.4	458.1/457.6	477.4/477.8	697.7/698.4	719.2/718.3
Reactivity (70gp) Loss	2.464	2.793	3.254	3.691	4.079	3.833	4.103
per Cycle (7gp) (%)	2.296	2.658	3.187	3.681	4.112	3.937	4.226
EOC Keff (70gp)	1.00997	1.00389	1.00025	1.00001	1.00062	1.00518	1.00585
(7gp)	1.00491	1.00523	1.00488	1.00467	1.00440	1.00490	1.00479
Pu (all) Burn	79.1	77.3	74.7	73.0	71.7	70.4	69.9
Rate (fissile) (Kg/TWhe)	96.1	97.0	97.3	97.5	97.6	100.9	101.0
Average Irradiation (GWd/te)	86.8	96.1	106.2	113.8	119.1	116.3	119.8

Table 6.12 High quality Pu: pin size x1.5, $ZrH_{1.7}$ & $^{10}B_4C$ as diluent, 6 month cycle

ZrH Fraction (pins)			86	53
B_4C Fraction (pins)			2	5
Pin Size			x1.5	x1.5
Pu (%)		(inner)	42.44	40.76
		(outer)	44.88	44.90
Na Void (%)			0.772	1.400
Doppler Constant			-.01055	-.00511
Void:Doppler Ratio			-73	-274
Inner/Outer Peak Linear Ratings (W/cm)	(A)	(BOC)	303.4/258.4	288.2/269.5
		(EOC)	269.3/269.5	272.1/272.3
	(B)	(BOC)	510.4/434.7	393.4/367.8
		(EOC)	453.0/453.4	371.4/371.6
Reactivity Loss per Cycle (%)		(70gp)	3.481	2.097
		(7gp)	3.583	2.205
EOC Keff		(70gp)	0.99016	1.01494
		(7gp)	1.00478	1.00486
Pu Burn Rate (Kg/TWhe)		(all)	68.7	71.4
		(fissile)	105.1	104.3
Average Irradiation (GWd/te)			112.6	90.0

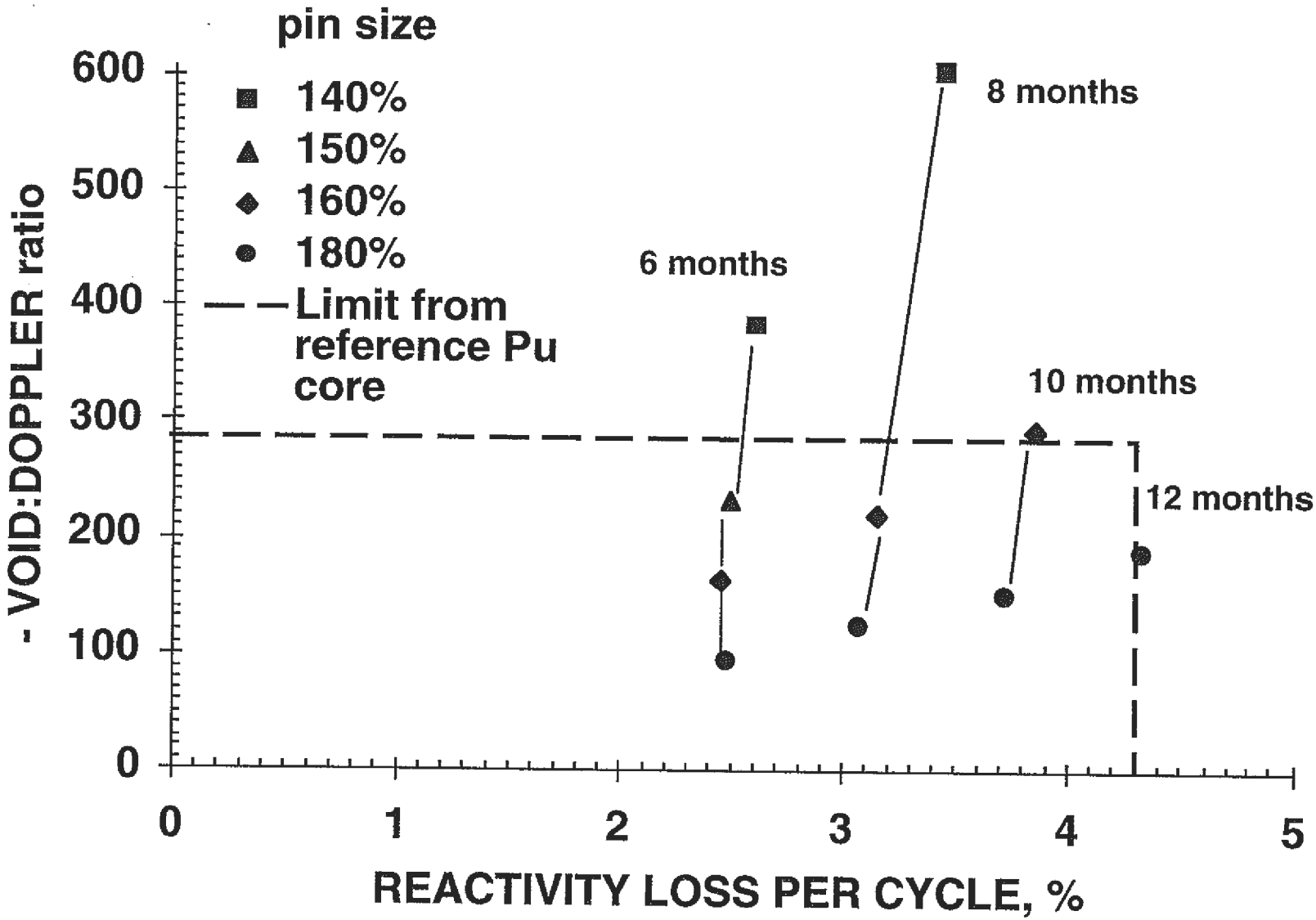

Fig. 6.1 Void:Doppler ratio as a function of reactivity loss per cycle, low quality Pu with $ZrH_{1.7}$ diluent

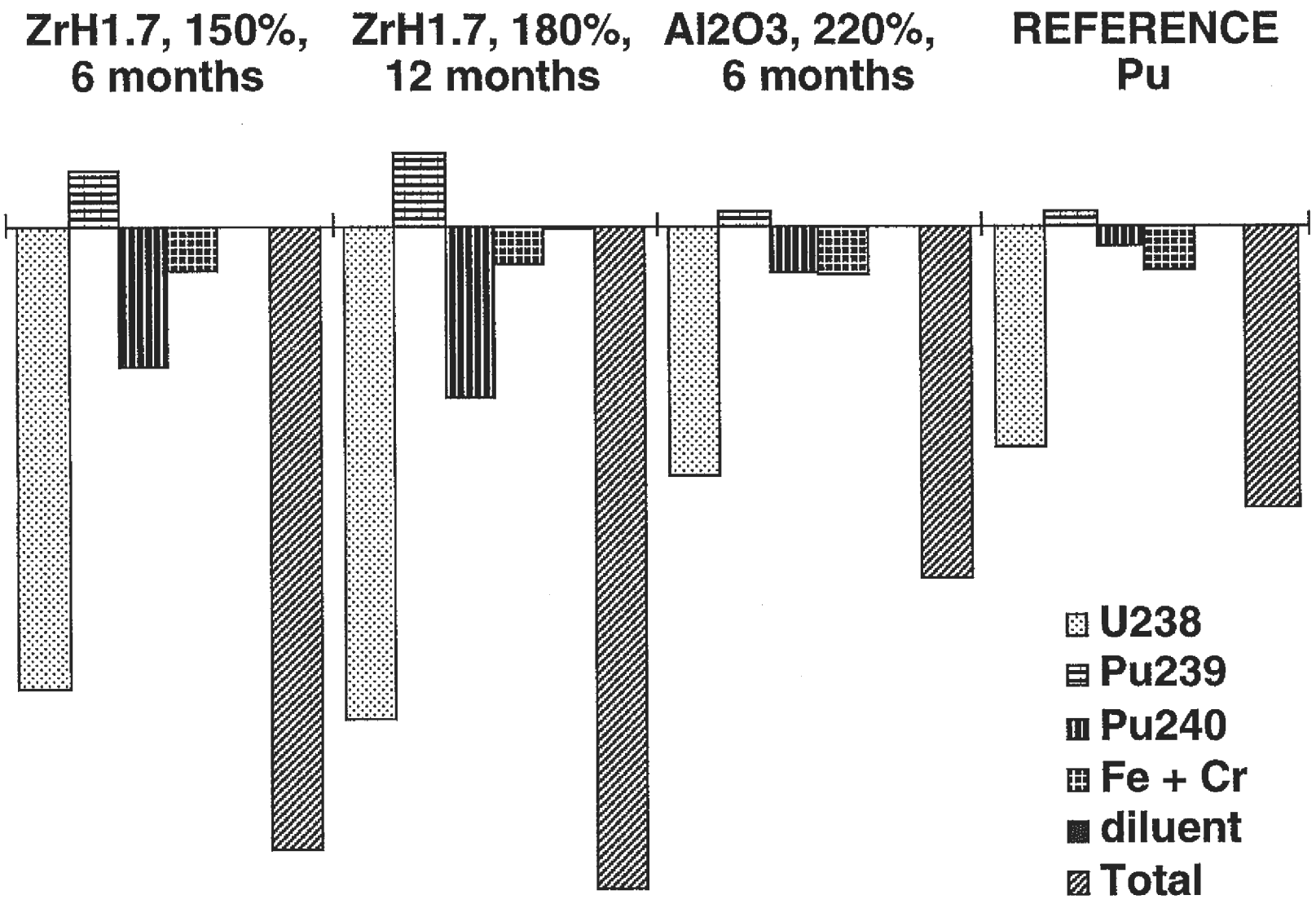

Figure 6.2 Main Doppler components, low quality Pu for various diluent materials, pin sizes and cycle lengths

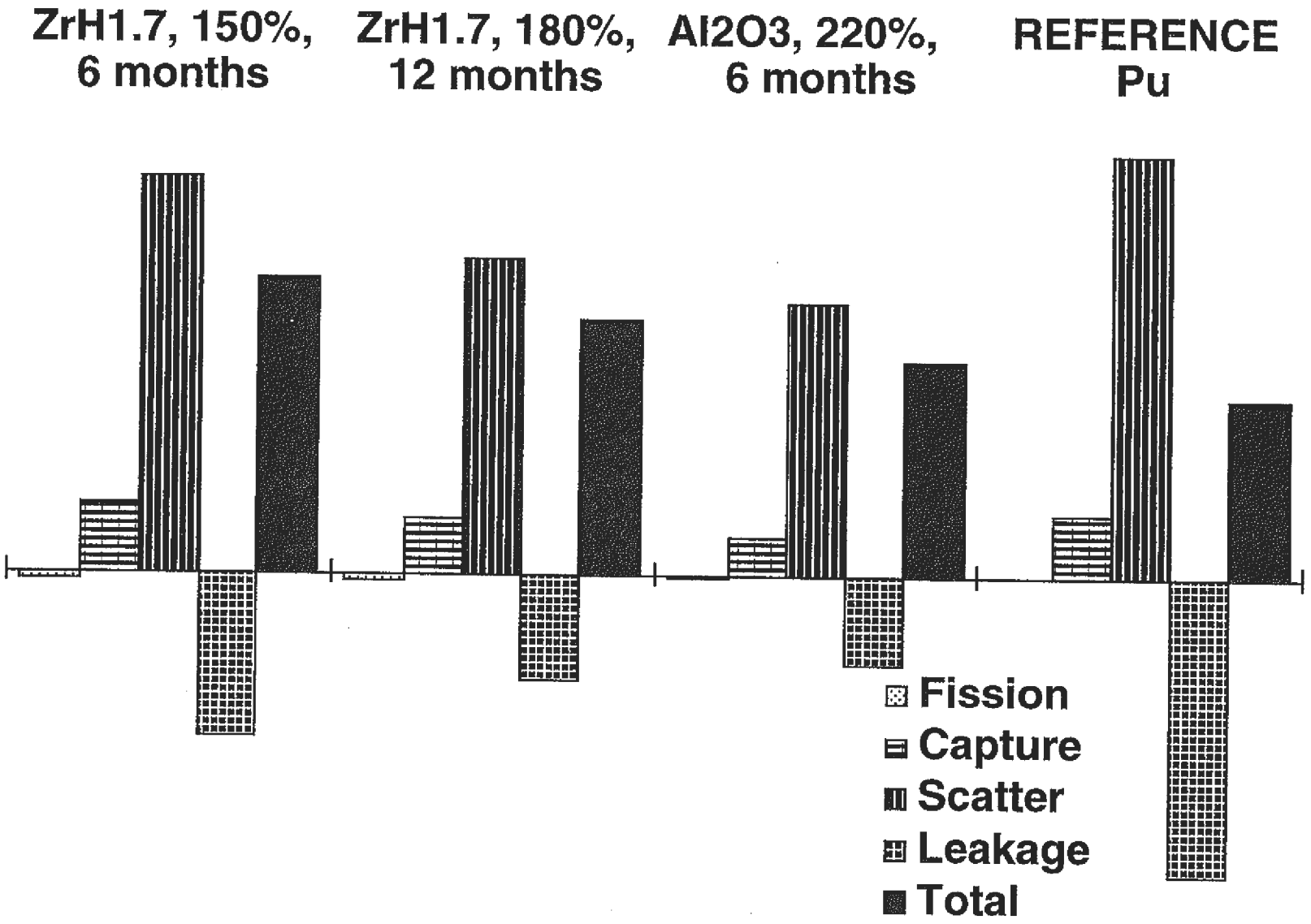

Fig. 6.3 Na void components, low quality Pu for various diluent materials, pin sizes and cycle lengths

7 DISCUSSION

The examination of the mesh size was limited to the axial mesh. It is likely that some further improvement in accuracy would result if the radial mesh at the outer edge of the core were refined. However, because of the 'pancake' shape of the core, any radial effect should be a lot smaller than the axial effect shown in Section 3.2.1. It would be appropriate to consider what was the effect of the coarser axial mesh adopted in earlier analyses (e.g. reference 1-10) on the values calculated, especially for Na void worth, and on the conclusions drawn.

The existence of a significantly enhanced thermal flux at the core edge has been observed. It is explicable in terms of the moderating effects of diluent within the core and of the shield material, together with the absence of a breeder blanket separating the core from the shield. A significant power fraction was produced by thermal fissions, though this was qualitatively different from that observed in calculations carried out elsewhere[3-11]. The differences may be a consequence of the presence of diluent S/As in the other calculations; alternatively, it may result from the use of different cross-section data libraries. The thermal region has been considered as comparatively unimportant in cross-section data for fast reactors, it may be that addressing uncertainties in such data would clarify the position with regard to thermal fission effects.

The PERKY perturbation calculations involve the summation of a large number of components. This has the potential to introduce errors into the calculations; this was particularly significant where the Na void worth was near zero as a result of large negative and positive components cancelling each other out; it could also be important in the calculation of 'by isotope' components of Doppler. Apart from the use of a finer group structure, another possibility for improving the accuracy of the PERKY calculations would be to alter the program variable length from single precision to double precision.

The value of reactivity loss per cycle assessed in the studies is not in itself a limiting parameter: it is, however, a principal component of the shutdown requirement and thus important when using

the rod worths to calculating the shutdown margins. Rod worth and shutdown margin values are produced by 3D calculations (thus they were beyond the scope of the current report). The reactivity loss gives a reasonable indication of the variation in shutdown margin, but 3D calculations are necessary to ascertain the effects of other factors. In particular, it is expected that the presence of absorber in the core as diluent will reduce the worth of the control rods. 3D calculations covering shutdown margins will be the subject of a further report; it is possible that they will indicate a requirement for a decreasing loss per cycle as the Pu quality improves.

The pin ratings produced by the calculations did not take into account a number of factors which will tend to increase the peak values. There are no control rod absorbers modelled, they will distort both axial and radial rating distributions. A uniform irradiation distribution is modelled, there will be significant variations between S/As, both radially and between different irradiation batches. The R-Z geometry modelled cannot fully represent the radial rating variations, both S/A-to-S/A and pin-to-pin; the partitioning of diluents in separate S/As or pins will exacerbate these effects. In opposition to the above effects, since the BOEC inner/outer zone ratings were not actively balanced, in many of the calculations the peak pin ratings were overestimated (by 1% to 20%). It is likely that at least some of the peak rating values will have been underestimated, though probably not by as much as the margins to the 430 W/cm limit that were commonly demonstrated; a more detailed calculational model and methods would be needed to produce more accurate values.

The use of a homogeneous lattice cell model to calculate macroscopic cross-sections was necessary to avoid explicitly specifying the positions of the diluent materials in the current sensitivity study. The extra complication of a more realistic heterogeneous cell model would only be justified for a more detailed in-depth study of a pre-defined design. Given the comparative nature of this study, the errors introduced by adopting a homogeneous model are not considered to be significant. It is noted that a heterogeneous calculation is necessary to investigate the differences between diluent being mixed in the fuel pellet and in separate pins,

other than the linear rating change associated with altering the number of fuelled pins.

The choice of material(s) to use for diluent is in part dependant upon factors beyond those assessed in this report. The inclusion of materials, other than 'void', within the fuel pellet raises many questions regarding chemical compatibility with the fuel and the thermal and mechanical properties of the resultant combination. A great deal of R&D would be required to validate the use of any such mixture. Even for diluent located in separate pins from the fuel, there are potential problems related to the mixing of absorber and non-absorber diluent materials. Some diluent materials, such as B_4C, have the advantage of already being proven as suitable materials for a fast reactor core.

There appears to be a definite benefit from adopting $ZrH_{1.7}$ as a non-absorbing diluent material. Given that the performance of this material diverged significantly from all the comparable materials assessed, it would be appropriate to ensure that the results are not a consequence of uncertainties in the cross-section data.

This study has given no consideration to the distribution of the diluent pins within the pin bundle of each S/A: since the lattice cell used a homogeneous model, the pin distribution was irrelevant to the calculations. In practise, the diluent pin positioning may have a significant impact on the thermo-hydraulic performance of the S/A, both directly from the fact that they are unfuelled pins and indirectly from their impact on the flux distribution (especially if absorber is concentrated in a very small number of pins). It is possible that thermo-hydraulic considerations will restrict the diluent pins to one of a limited number of patterns with specific numbers of pins. If this is so then it would be possible to achieve intermediate diluent fractions by including a limited amount of voidage in the fuel pellets (either as a density reduction, or as hollow pellets). Figure 7.1 shows a number of symmetric patterns of diluent pin positioning for a 217 pin S/A.

There are three options for positioning diluent materials in the core: within fuel pellets; in separate pins within each S/A; in separate S/As. It was considered that the current study was a

reasonable approximation to the first two options. Diluent S/As would produce a distortion in the radial flux distribution that would only be properly modelled by a 3D calculation, as such they were beyond the scope of this study. The self-shielding effect of placing diluent in separate S/As would increase the dilution fraction required beyond those encountered in this study - this may result in difficulties in achieving the 430 W/cm rating limit.

Since it was necessary to adjust the pin size in order to achieve a viable core with the low quality Pu, it can be concluded that in optimizing the Pu burning core design the lowest quality Pu should have been considered in defining the fuel fraction.

The refinement of the axial mesh and different calculational route caused significant changes to the values of key parameters from those of the reference Pu core as optimised in reference 1-10. This raised the question of whether the resulting values remained suitable for use as target values. The Na void worth changed from 1.01% to 1.63% and the Doppler constant from -0.00429 to -0.00573, altering their ratio from -235 to -285. At the same time the reactivity loss per cycle was reduced from 4.72% to 4.30%. From Figure 5.8 it can be concluded that the calculations of this study would have produced similar margins to the target whichever of the two sets of key parameters was adopted for that role.

The analysis of the results did not take into account the fraction of the calculated Doppler coefficient that was associated with structural materials - the temperatures of these materials will lag behind that of the fuel, effectively reducing the Doppler coefficient. The fraction of Doppler from the structure increases from ~15% to ~17% to ~21% as the Pu quality varies from low to reference to high. The differences between these values indicate that adjusting the analysis to exclude the structural component would not have affected the results greatly. With $ZrH_{1.7}$ as diluent the fractions of Doppler coming from structural materials were approximately half the values given above: this represents an unacknowledged further improvement in those cases where $ZrH_{1.7}$ diluent was used.

The core variant of adopting a 45% uniform Pu enrichment, balancing the S/A ratings between the inner and outer core zones by use of diferential diluent fractions, increased the rate of Pu burning by ~6%. This was achieved at the expense of an increased rating in the inner core zone (assuming the diluent was not mixed in the fuel pellets). The higher the Pu quality the lower will be the margin available to the 430 W/cm pin rating limit. Thus the use of a uniform Pu enrichment is more likely to be feasible the lower the quality of the Pu vector - this is advantageous since there is some reduction in the Pu burning rate as the Pu quality reduces.

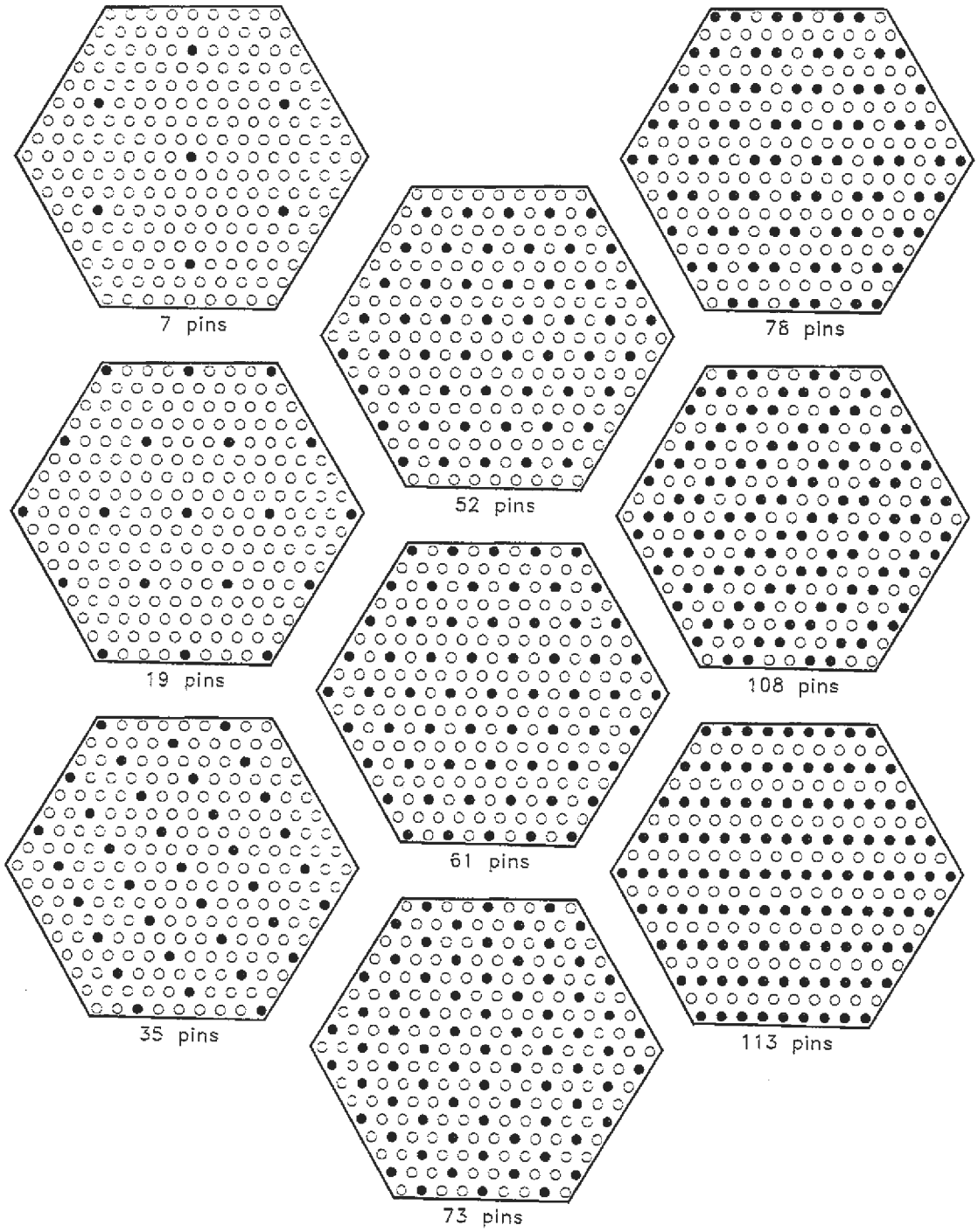

Fig. 7.1 Potential diluent pin patterns for a 217 pin S/A

8 CONCLUSIONS

It proved possible to produce a single design for a 600 MWe Pu burning fast reactor core that is capable of burning a wide range of Pu compositions. Pu vectors varying from high grade military to the product of multiple recycling in a Pu burner have been successfully incorporated in a single core design. It was possible to maintain values for key parameters - reactivity loss per cycle, Na void and Doppler related safety parameters - that were no worse than those of a core design optimized for burning Pu of an intermediate quality[1-10].

The initial core design examined, based on the intermediate (reference) quality Pu, had to be modified to be acceptable to the low quality (multi-recycled) Pu - the pin size and fuel volume fraction had to be increased (by a factor from x1.4 to x2.2). When designing a Pu burning core, the lowest quality Pu vector to be used should be taken into account when defining the fuel volume fraction.

Various materials were examined as diluents replacing a fraction of the fuel; they were used to adjust the core reactivity, and also to adjust values of the key parameters. The use of absorber ($^{10}B_4C$) caused the reactivity loss per cycle to improve (reduce), whilst the Na void and Doppler safety parameters worsened. Void, transparent or moderating diluent caused the reactivity loss to increase but the safety parameters to improve. An optimized mixture of absorber and another material as diluent allows the effects on these key parameters to be balanced (for the low quality Pu core, no absorber was necessary).

There was a definite preference for the use of $ZrH_{1.7}$ as the non-absorbing diluent. With this material there was no problem in achieving the target values for key parameters for all three Pu vectors and using the reference conditions of a 45% peak Pu enrichment and irradiation in 4 batches with a 6 month cycle. This was achieved with an increased pin size of x1.5, corresponding to core volume fractions of - steel: 19.9%, coolant: 51.3%, fuel and diluent: 24.3%. If the low quality Pu fuel cycle length was reduced to 3 batches of 6 months, a pin size increase to ~x1.4 would be possible. In all these cases it was possible to maintain a margin of

at least 10% to a 430 W/cm linear rating limit, whether the diluent was considered to be mixed in the fuel pellets or in separate pins. The adoption of a larger pin size would allow a longer irradiation cycle to be used for at least some Pu qualities, but at the expense of some increase in pin ratings: a x1.8 pin size would allow a 12 month cycle for the low quality Pu.

There was comparatively little to choose between the other non-absorber diluents examined, $^{11}B_4C$ and BeO were both marginally better than CeO_2, MgO, Al_2O_3 or 'void'. There are practical advantages to the use of $^{11}B_4C$, since both the absorber and non-absorber diluents are then the same chemical material. Calculations were done using B_4C as diluent, the ^{10}B fraction determining the absorber-moderator balance; there was generally enough margin in the results to make them applicable to all the non-absorber diluents, not just $^{11}B_4C$. To achieve criticality an increased pin size of ~x2.2 was required. It was again possible to achieve the target values of reactivity loss and Na void and Doppler safety parameters. The larger pin size (compared with $ZrH_{1.7}$ moderator) results in significantly higher pin ratings: with the diluent in separate pins from the fuel, a 430 W/cm limit is just reached for the low quality Pu and greatly exceeded for the other Pu vectors. In order for the rating limit to be achieved, a significant fraction (at least 62%) of the diluent would have to be incorporated in fuel pellets. One method of achieving this would be by adopting hollow fuel pellets, thus incorporating 'void' as diluent.

Thus, it was necessary either to employ $ZrH_{1.7}$ as a diluent material or else for at least part of the diluent material used to be incorporated into the fuel pellets. In the latter case it is possible for the diluent within the fuel pellets to be provided by an increased voidage, possibly in the form of hollow pellets.

A core variant was studied, with a uniform Pu enrichment of 45% and the rating balance between inner and outer core zones maintained by adopting different diluent fractions in the two zones. This has the advantage of increasing the Pu burning rates by ~6% relative to the more normal assumption of a uniform diluent fraction. It is only possible to adopt this variation where there is some margin to pin

rating limits, since it requires the addition of extra diluent in the inner core zone.

The presence of $^{10}B_4C$ absorber as diluent will tend to reduce the worth of the absorber rods, it is therefore necessary to assess shutdown margins for Pu burner cores with diluent. The current calculations have used 2D R-Z geometry; rod worths and shutdown margins have not been assessed since these require 3D calculations. Shutdown margins will be the subject of a future report.

An assessment of the axial mesh showed a requirement for a finer mesh than normal if axial effects, especially Na void worth, were to be properly modelled in a high axial leakage 'pancake' core design.

Appreciable thermal fission effects were discovered, associated with the absence of breeder regions at the core edge and the inclusion of diluent materials. The effects are qualitatively different from those seen elsewhere[3-11] in Pu burning cores, possibly due to differences in cross-section data in the thermal region. It would be appropriate to undertake further investigation of the cause of these differences.

The results of this study support the concept of using a single reactor design to burn the full range of Pu qualities. However, in addition to the 3D shutdown margin calculations mentioned above, there are a number of other areas in which further work is indicated to ascertain the practicability of the approaches examined in this report:

the compatability of absorber ($^{10}B_4C$) mixed with other diluent materials (especially $ZrH_{1.7}$) in the same pin

the incorporation of diluent material within the fuel pellets

the use of hollow or reduced density fuel pellets

flow restrictors or other design options to produce S/As with the same thermo-hydraulics but different size fuel pellets

in-channel rating distribution with unfuelled pins, including pure $^{10}B_4C$ pins

thermo-hydraulic effects of unfuelled pins in a S/A

review $ZrH_{1.7}$ cross-section data.

Depending on the results of the above, it may prove necessary to consider the use of diluent S/As; that would require the use of 3D calculations.

ACKNOWLDGEMENT

The author wishes to express his thanks to PNC for being given the opportunity under the International Fellowship scheme to come to work in Japan and undertake the task reported herein.

The work was carried out under the supervision of the General Manager of the Reactor Physics Research Section, Dr, Wakabayashi, who provided the right level of support to allow the task to be carried out in an effective and rewarding manner. Both Dr. Wakabayashi and the Deputy General Manager of the Reactor Physics Research Section, Mr. Ishikawa, participated in technical discussions which were essential to guiding the direction of the work as it progressed.

The work would have been immeasurably more onerous, if not impossible, without the willing contributions of all the members of the Reactor Physics Research Section, in helping me understand the various computer systems and programs used, and particularly in facilitating access to various Japanese reports and data sources.

REFERENCES

1-1 M.Yamaoka, M.Ishikawa, T.Wakabayashi. Feasibility study of TRU transmutation by LMFBRs. Proc. Int. Conf. on Fast Reactors and Related Fuel Cycles (FR'91), Vol.IV, Oct.28-Nov.1, Kyoto (1991)

1-2 T.Wakabayashi, M.Yamaoka, M.Ishikawa, H.Hirao. Status of study on TRU transmutation in LMFBRs. Trans. Am. Nucl. Soc., 64, 556 (1992)

1-3 M.Yamaoka, T.Wakabayashi. Design study of a super long life core loaded with TRU fuel. Proc. Int. Conf. on design and safety of advanced nuclear power plants (ANP'92), Vol.I, Oct.25-29, Tokyo (1992)

1-4 T.Wakabayashi, T.Ikegami. Characteristics of an LMFBR core loaded with minor actinide and rare earth containing fuels. Proc. Int. Conf. on Future Nuclear Systems: Emerging Fuel Cycles and Waste Disposal Options (GLOBAL'93), Vol.1, Sep.12-17, Seattle (1993)

1-5 T.Wakabayashi, S.Okhi, T.Ikegami. Feasibility studies of an optimized fast reactor core for MA and FP transmutation. Proc. Int. Conf. on Evaluation of Emerging Nuclear Fuel Cycle Systems (GLOBAL'95), Vol.I, Sep.11-14, Versailles (1995)

1-6 L.Koch. Formation and recycling of minor actinides in nuclear power stations, Handbook on the physics and chemistry of the actinides, Chapter 9. North-Holland publishing (1986)

1-7 Committee on International Security and Arms Control, US National Academy of Sciences, Management and disposition of excess weapons plutonium. National Academy Press (1994)

1-8 A.Languille et al. CAPRA core studies - the oxide reference option. Proc. Int. Conf on Evaluation of Emerging Nuclear Fuel Cycle Systems (GLOBAL'95), Vol.I, Sep.11-14, Versailles (1995)

1-9 J.C.Garnier, A.Shono, T.Wakabayashi. Parametrical Studies on Pu burning in fast reactors. Proc. Int. Conf. on Evaluation of Emerging Nuclear Fuel Cycle Systems (GLOBAL'95), Vol.I, Sep.11-14, Versailles (1995)

1-10 M.Yano et al. An evaluation of core characteristics of the Pu burning by LMFRs (II). PNC PJ9678 95-002 (1995)

1-11 PNC - CEA collaboration meeting report (1995/4/10-12, at Oarai Engineering Center). PNC ZN9100 95-005 (1995)

1-12 T.Wakabayashi, K.Takahashi, T.Yanagisawa. Feasibility studies on Pu and minor actinide burning in fast reactors. (to be published)

2-1 A.Hara, M.Katsumata, S.Aoyagi. Manual for PENCIL code system. PNC SN9520 89-008 (1989)

3-1 A.Shono, K.Hiyama. Calculational method for actinide burning core design. PNC PN9520 94-003 (1994)

3-2 M.Nakagawa, K.Tsuchihashi. SLAROM: A code for cell homogenization calculation of fast reactor. JAERI 1294 (1984)

3-3 T.B.Fowler et al. Nuclear reactor core analysis code: CITATION ORNL-TM-2496, Rev. 2 (1971)

3-4 S.Iijima, H.Yoshida, H.Sakuragi. Calculation program for fast reactor design, 2 (Multi-dimensional perturbation theory code based on diffusion approximation: PERKY). JAERI-M 6993 (1977)

3-5 M.Nakagawa, J.Abe. Code system for fast reactor neutronics analysis. JAERI-M 83-066 (1983)

3-6 K.Kinjo et al. Design study on large scale fast breeder reactor - 1,000 MWe size reference plant. PNC ZN9410 89-171 (1989)

3-7 T.Nakagawa, T.Asami, T.Yoshida. Curves and tables of neutron cross sections - Japanese Evaluated Nuclear Data Library version 3. JAERI-M 90-099 (1990) (under revision)

3-8 L.Tomlinson. AERE-R6993

3-9 M.C.Brady et al. NSE, 103, 129 (1989)

3-10 D.Saphier et al. Evaluated Delayed Neutron Spectra and Their Importance in Reactor Calculations. NSE, 62, 660 (1977)

3-11 K.G.Allen, H.M.Beaumont, S.N.Hunter. Reactor physics studies on the high burn-up version of the CAPRA 04.94 core. (NNC Ltd., for the CAPRA project) FR/E/004615A (1994)

3-12 JEF-PC A personal computer program for displaying nuclear data from the Joint Evaluated File library. OECD Nuclear Energy Agency (1994)

4-1 T.Nakagawa. Summary of JENDL-2 general purpose file JAERI-M 84-103 (1984)